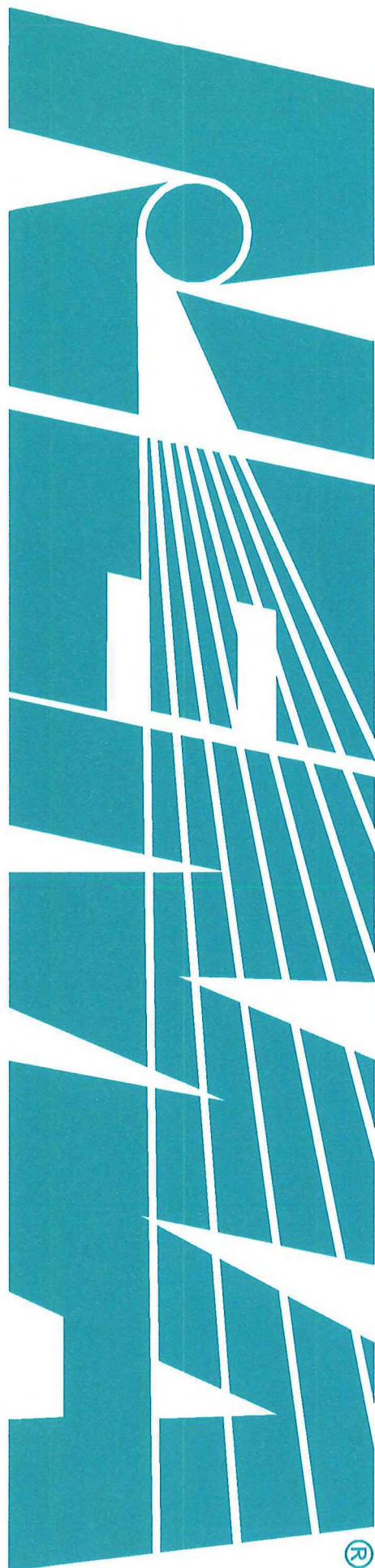


NEMA NU 2-2018

# Performance Measurements of Positron Emission Tomographs (PET)





## **NEMA Standards Publication NU 2-2018**

*Performance Measurements of Positron Emission Tomographs (PET)*

*Published by:*

**National Electrical Manufacturers Association**  
1300 N. 17<sup>th</sup> Street, Suite 900  
Rosslyn, VA 22209

[www.nema.org](http://www.nema.org)

© 2018 National Electrical Manufacturers Association. All rights including translation into other languages, reserved under the Universal Copyright Convention, the Berne Convention for the Protection of Literary and Artistic Works, and the International and Pan American Copyright Convention.

## NOTICE AND DISCLAIMER

The information in this publication was considered technically sound by the consensus of persons engaged in the development and approval of the document at the time it was developed. Consensus does not necessarily mean that there is unanimous agreement among every person participating in the development of this document.

The National Electrical Manufacturers Association (NEMA) standards and guideline publications, of which the document contained herein is one, are developed through a voluntary consensus standards development process. This process brings together volunteers and/or seeks out the views of persons who have an interest in the topic covered by this publication. While NEMA administers the process and establishes rules to promote fairness in the development of consensus, it does not write the document and it does not independently test, evaluate, or verify the accuracy or completeness of any information or the soundness of any judgments contained in its standards and guideline publications.

NEMA disclaims liability for any personal injury, property, or other damages of any nature whatsoever, whether special, indirect, consequential, or compensatory, directly or indirectly resulting from the publication, use of, application, or reliance on this document. NEMA disclaims and makes no guaranty or warranty, express or implied, as to the accuracy or completeness of any information published herein, and disclaims and makes no warranty that the information in this document will fulfill any of your particular purposes or needs. NEMA does not undertake to guarantee the performance of any individual manufacturer or seller's products or services by virtue of this standard or guide.

In publishing and making this document available, NEMA is not undertaking to render professional or other services for or on behalf of any person or entity, nor is NEMA undertaking to perform any duty owed by any person or entity to someone else. Anyone using this document should rely on his or her own independent judgment or, as appropriate, seek the advice of a competent professional in determining the exercise of reasonable care in any given circumstances. Information and other standards on the topic covered by this publication may be available from other sources, which the user may wish to consult for additional views or information not covered by this publication.

NEMA has no power, nor does it undertake to police or enforce compliance with the contents of this document. NEMA does not certify, test, or inspect products, designs, or installations for safety or health purposes. Any certification or other statement of compliance with any health or safety-related information in this document shall not be attributable to NEMA and is solely the responsibility of the certifier or maker of the statement.

## CONTENTS

|  |           |
|--|-----------|
| Foreword.....  | iv        |
| <b>Section 1 Definitions, Symbols, and Referenced Publications .....</b> | <b>1</b>  |
| 1.1 Definitions .....  | 1         |
| 1.2 Standard Symbols .....   | 1         |
| 1.3 Referenced Publications.....   | 3         |
| <b>Section 2 General .....</b>   | <b>4</b>  |
| 2.1 Purpose .....  | 4         |
| 2.2 Purview .....  | 4         |
| 2.3 Units of Measure .....   | 5         |
| 2.4 Consistency .....  | 5         |
| 2.5 Equivalency .....  | 5         |
| <b>Section 3 Spatial Resolution .....</b>                                | <b>7</b>  |
| 3.1 General .....  | 7         |
| 3.2 Purpose .....  | 7         |
| 3.3 Method.....  | 7         |
| 3.3.1 Radionuclide .....   | 7         |
| 3.3.2 Source Distribution .....  | 7         |
| 3.3.3 Data Collection .....  | 8         |
| 3.3.4 Data Processing .....  | 8         |
| 3.4 Analysis .....   | 8         |
| 3.5 Report.....  | 9         |
| <b>Section 4 Scatter Fraction, Count Losses, and Randoms .....</b>       | <b>10</b> |
| 4.1 General.....   | 10        |
| 4.2 Purpose .....  | 10        |
| 4.3 Method.....  | 10        |
| 4.3.1 Symbols .....  | 11        |
| 4.3.2 Radionuclide .....   | 11        |
| 4.3.3 Source Distribution .....  | 11        |
| 4.3.4 Data Collection .....  | 12        |
| 4.3.5 Data Processing .....  | 12        |
| 4.4 Analysis .....   | 13        |
| 4.4.1 Analysis with Randoms Estimate .....                               | 14        |
| 4.4.2 Alternative Analysis with No Randoms Estimate .....                | 15        |
| 4.5 Report.....  | 16        |
| 4.5.1 Count Rate Plot .....  | 16        |
| 4.5.2 Peak Count Values.....   | 16        |
| 4.5.3 System Scatter Fraction .....                                      | 16        |
| 4.5.4 Table and Phantom Positioning, and Projection Alignment .....      | 16        |
| <b>Section 5 Sensitivity.....</b>  | <b>17</b> |
| 5.1 General .....  | 17        |
| 5.2 Purpose .....  | 17        |
| 5.3 Method.....  | 17        |
| 5.3.1 Symbols .....  | 17        |
| 5.3.2 Radionuclide .....   | 17        |
| 5.3.3 Source Distribution .....  | 18        |
| 5.3.4 Data Collection .....  | 18        |
| 5.4 Calculations and Analysis.....                                       | 18        |
| 5.4.1 System Sensitivity .....   | 18        |
| 5.4.2 Axial Sensitivity Profile .....                                    | 19        |
| 5.5 Report.....  | 19        |

|  |           |
|--|-----------|
| <b>Section 6 Accuracy: Corrections for Count Losses and Randoms .....</b>    | <b>21</b> |
| 6.1 General .....  | 21        |
| 6.2 Purpose .....  | 21        |
| 6.3 Method .....   | 21        |
| 6.3.1 Symbols .....  | 21        |
| 6.3.2 Radionuclide .....   | 21        |
| 6.3.3 Source Distribution .....  | 21        |
| 6.3.4 Data Collection .....  | 21        |
| 6.3.5 Data Processing .....  | 21        |
| 6.4 Analysis .....   | 21        |
| 6.5 Report .....   | 22        |
| <b>Section 7 Image Quality, Accuracy of Corrections .....</b>                | <b>23</b> |
| 7.1 General .....  | 23        |
| 7.2 Purpose .....  | 23        |
| 7.3 Method .....   | 23        |
| 7.3.1 Symbols .....  | 23        |
| 7.3.2 Radionuclide .....   | 23        |
| 7.3.3 Source Distribution .....  | 24        |
| 7.3.4 Data Collection .....  | 24        |
| 7.3.5 Data Processing .....  | 25        |
| 7.4 Analysis .....   | 25        |
| 7.4.1 Image Quality .....  | 25        |
| 7.4.2 Accuracy of Corrections .....  | 26        |
| 7.5 Report .....   | 26        |
| <b>Section 8 Time-of-Flight Resolution .....</b>                             | <b>30</b> |
| 8.1 General .....  | 30        |
| 8.2 Purpose .....  | 30        |
| 8.3 Method .....   | 30        |
| 8.3.1 Symbols .....  | 30        |
| 8.3.2 Radionuclide .....   | 31        |
| 8.3.3 Source Distribution .....  | 31        |
| 8.3.4 Data Collection .....  | 31        |
| 8.3.5 Data Processing .....  | 31        |
| 8.4 Analysis .....   | 32        |
| 8.4.1 2-D Histogram formation .....  | 32        |
| 8.4.2 Scatter and Random Removal .....                                       | 33        |
| 8.4.3 FWHM Analysis .....  | 33        |
| 8.5 Report .....   | 33        |
| <b>Section 9 PET-CT Coregistration Accuracy.....</b>                         | <b>35</b> |
| 9.1 General .....  | 35        |
| 9.2 Purpose .....  | 35        |
| 9.3 Method .....   | 35        |
| 9.3.1 PET-CT Fiducial Marker .....   | 35        |
| 9.3.2 Fiducial Marker and Mass Distribution .....                            | 35        |
| 9.3.3 Data Collection .....  | 36        |
| 9.3.4 Data Processing .....  | 37        |
| 9.4 Analysis .....   | 37        |
| 9.4.1 PET and CT Image Fusion .....  | 37        |
| 9.4.2 Processing of Data .....   | 37        |
| 9.4.3 Location of Maximum Voxel Value in the PET and CT Data.....            | 37        |
| 9.4.4 Dimensions of the Volume Used in the Calculation of the Centroid ..... | 38        |
| 9.4.5 PET and CT Centroids .....   | 39        |
| 9.4.6 Verification of Fiducial Marker Dimension and Pixel Size .....         | 39        |

|     |                                  |    |
|-----|----------------------------------|----|
| 9.5 | 9.4.7 Coregistration Error ..... | 40 |
|     | Report.....                      | 41 |

## Foreword

### Reason for Changes

NEMA requires that its standards be reviewed and, if necessary, updated every five years. This standards publication was developed by the NU 2 Task Force chartered by the Molecular Imaging Section of MITA. Committee approval of the standard does not necessarily imply that all committee members voted for its approval or participated in its development. The task force was composed of the following members:

Yanic Bercier—Siemens Healthineers, Knoxville, TN  
Michael A. Miller—Philips, Highland Heights, OH  
Charles W. Stearns—GE Healthcare, Waukesha, WI  
Jeffrey Kolthammer—Canon Medical, Vernon Hills, IL

In the preparation of this standards publication, input of users and other interested parties has been sought and evaluated. Inquiries, comments, and proposed or recommended revisions should be submitted to the concerned NEMA product section by contacting the:

Senior Technical Director, Operations  
National Electrical Manufacturers Association  
1300 North 17<sup>th</sup> Street, Suite 900  
Rosslyn, Virginia 22209

### Changes to Tests

The changes made by the Task Force from the 2012 version of this standard include the addition of two new sections:

- a. Section 8, to assess the coincidence timing resolution of time-of-flight PET systems, and
- b. Section 9, to assess the co-registration accuracy of hybrid PET/CT systems.

Other changes to the current version are relatively minor, mostly designed to make the tests easier to conduct, more reproducible, more clearly defined, or better harmonized with other performance tests. These are the most substantial changes to the tests (note that this is not intended to be an exhaustive list):

- a. In Section 3, the spatial resolution test allows <sup>22</sup>Na as well as <sup>18</sup>F.
- b. In Section 3, the spatial resolution test point source is specified in terms of point source dimensions as opposed to capillary tube dimensions. The capillary tube is specified as an option.
- c. In Section 4 (and in Section 6 and Section 8, which use the same acquired data), the test phantom is to be positioned so that the trough of the table is positioned  $15 \pm 1$  cm below the center of the transverse field of view (FOV).
- d. In Section 6, the analysis is to be conducted over the central 80% of the PET axial FOV.
- e. In Section 7, the 28 mm and 37 mm diameter cold spheres are replaced with 28 mm and 37 mm diameter hot spheres. All six spheres are to be hot.
- f. In Section 7, there is no option for a hot sphere-to-background fill ratio of 8:1.
- g. In Section 7, the lung residual error analysis excludes slices that are within 30 mm of the axial edge of the lung insert; the previous value was 10 mm.
- h. In Section 7, the description of phantom positioning is clarified. If the patient table cannot center the body phantom lung insert, adjust the patient table height to center the phantom as closely as possible. The phantom shall not be elevated above the patient table surface in order to center the phantom lung insert.

## Scope

The philosophy and rationale of the standards measurements and illustrative examples of the analysis and results are presented in

*Journal of Nuclear Medicine*, vol. 43, no. 10, 2002. Daube-Witherspoon ME, Karp JS, Casey ME, DiFilippo FP, Hines H, Muehllehner G, Simcic V, Stearns CW, Adam L-E, Kohlmyer S and Sossi V. "PET Performance Measurements Using the NEMA NU 2-2001 Standard." pp. 1398-1409.

With the exceptions of Section 8 for time-of-flight systems and Section 9 for hybrid PET/CT systems, the Task Force has attempted to specify methods that can be performed on all positron emission tomographs. These include single and multiple slice, discrete and continuous detector, time-of-flight instruments, multi-planar and volume reconstruction models, and dedicated positron emission tomographs as well as other coincidence-capable imaging systems. Wherever possible, future developments that could be readily anticipated were taken into account.

While many PET tomographs are constructed as hybrid imaging systems such as PET/CT and PET/MR systems, the standards committee has not specified special methods to assess hybrid imaging performance with the exception of the PET/CT registration test described in Section 9. It is expected that the PET component of a hybrid imaging system can be assessed using the methods described in this standard, and other portions of the system can be assessed using other standards appropriate to that technology. The method for assessing the co-registration accuracy of hybrid PET/CT systems has the potential to be adapted to PET/MR systems. In the event a portion of any of the PET test methods described here cannot be executed in a hybrid imaging system, workaround methods may be used, but those methods must be described in the test report.

< This page is intentionally left blank. >

## Section 1

### Definitions, Symbols, and Referenced Publications

#### 1.1 Definitions

**axial field of view (FOV):** The maximum length parallel to the long axis of a positron emission tomograph along which the instrument generates transaxial tomographic images.

**full-width at half-maximum (FWHM):** A measure of spread of a distribution given by the difference between points where the value reaches half the maximum value.

**line of response (LOR):** The line in 3-D space formed by a coincidence event's two-end detected points.

**list-mode:** A correlated projection data file format where each coincidence event is listed sequentially, parameter by parameter. For the purposes of this standard, the list mode data is assumed to include information describing the spatial position of the LOR, and, if the data is acquired in a time-of-flight (TOF) mode, the TOF information about each recorded coincidence event.

**prompt counts:** Coincidence events acquired in the standard coincidence window of a positron emission tomograph. Prompt counts include true, scattered, and random coincidence events.

**sinogram:** A two-dimensional representation of projection space data, where one dimension refers to radial distance from the center, and the second dimension refers to projection angle.

**time-of-flight (TOF):** Arrival time difference of two photons in a coincidence event, from which the annihilation point along the LOR can be estimated.

**transverse field of view (FOV):** The maximum diameter circular region perpendicular to the long axis of a positron emission tomograph within which objects might be imaged.

**test phantom:** Components for each measurement are defined in the description of that measurement.

#### 1.2 Standard Symbols

Symbolic expressions for certain quantities are used throughout this standards publication. Symbols that use any one of the standard subscripts to specify further a basic quantity are identified by the subscript string "xxx." Symbols which represent quantities that are indexed over a series of acquisitions and/or each slice in an image or data set may have that indexing identified by further subscript strings such as ",j," or ",jj" as defined in the related text. All quantities expressed as a function of some independent variable shall be symbolically represented as  $Q(x)$ , where  $x$  is a lower-case letter representing the variable as defined in the related text.

**counts ( $C_{xxx}$ ):** The number of coincidence events:

- a.  $C_{ROI}$  – events in a planar region of interest
- b.  $C_{TOT}$  – total number of events
- c.  $C_{r+s}$  – random plus scatter event count
- d.  $C_L$  – event count at left edge of projection area of interest
- e.  $C_R$  – event count at right edge of projection area of interest
- f.  $C_H$  – counts in a hot region of interest

- g.  $C_B$  – counts in a background region of interest

**radioactivity ( $A_{xxx}$ ):** A nuclear decay rate in units of megabecquerels (MBq), i.e., in units of 1 million disintegrations per second, and optionally expressed in units of millicuries (mCi), i.e., in units of 37 million disintegrations per second:

- $A_{cal,meas}$  – radioactivity at time  $T_{cal}$ , as measured in the dose calibrator
- $A_{cal}$  – line source radioactivity corrected for source length
- $A_{ave}$  – average radioactivity during an acquisition

The average radioactivity for a particular acquisition at starting time  $T$  shall be computed using the corrected line source activity,  $A_{cal}$ , as measured at  $T_{cal}$ , the half-life of the radionuclide,  $T_{1/2}$ , and the duration of the acquisition,  $T_{acq}$ , according to:

$$A_{ave} = A_{cal} \left( \frac{T_{1/2}}{T_{acq} \ln 2} \right) \exp \left( \ln 2 \frac{T_{cal} - T}{T_{1/2}} \right) \left[ 1 - \exp \left( -\ln 2 \frac{T_{acq}}{T_{1/2}} \right) \right].$$

**radioactivity concentration ( $a_{xxx}$ ):** A nuclear decay rate per unit volume in units of kilobecquerels per milliliter (kBq/ml), i.e., in units of 1 thousand decays per second per milliliter, and optionally expressed in units of microcuries per milliliter ( $\mu\text{Ci}/\text{mL}$ , i.e., in units of 37 thousand decays per second per milliliter):

- $a_{t,peak}$  – radioactivity concentration at peak true event rate
- $a_{eff}$  – effective average activity concentration of a line source in a solid cylinder
- $a_H$  – radioactivity concentration in a hot sphere
- $a_B$  – radioactivity concentration in the background
- $a_{NEC,peak}$  – radioactivity concentration at the peak NECR rate

The radioactivity concentration of a quantity of radioactivity distributed uniformly through a volume  $V$  shall be found by dividing the activity,  $A_{xxx}$ , by the volume  $V$  within which the activity is uniformly distributed, according to:

$$a_{xxx} = \left( \frac{A_{xxx}}{V} \right)$$

The average radioactivity concentration is thus

$$a_{ave} = \left( \frac{A_{ave}}{V} \right)$$

Note that in computing the effective radioactivity concentration,  $a_{eff}$ , the volume to be used is the volume of the solid cylinder, not the volume of its line source insert.

**radioisotopic half-life ( $T_{1/2}$ ):** The interval of time during which half of the nuclei of a radionuclide are likely to decay. For the nuclide  $^{18}\text{F}$ , the half-life is 1.8295 hours (i.e., 109.77 minutes or 6586.2 seconds; Reference: NIST Standard Reference Database 120), but the value of 1.830 hours (or 109.8 minutes or 6588 seconds) used in previous versions of this standard may continue to be used with negligible impact on measured results.

**rate ( $R_{xxx}$ ):** A coincidence event rate measured in events per second, defined as the coincidence counts divided by the time interval  $T_{acq}$ :

- $R_{ROI}$  – rate in a planar region of interest
- $R_{TOT}$  – total event rate

- c.  $R_{\text{Fit}}$  – fit event rate
- d.  $R_t$  – true event rate
- e.  $R_s$  – scatter event rate
- f.  $R_r$  – random event rate
- g.  $R_{t,\text{peak}}$  – peak true event rate
- h.  $R_{\text{NEC}}$  – noise equivalent count rate
- i.  $R_{\text{NEC,peak}}$  – peak noise equivalent count rate
- j.  $R_{\text{CORR}}$  – decay-corrected count rate

**time ( $T_{xxx}$ ):** A time measured in seconds:

- a.  $T_{\text{acq}}$  – duration of an acquisition
- b.  $T_j$  – starting time of acquisition  $j$
- c.  $T_{\text{cal}}$  – time of well counter measurement

**volume ( $V$ ):** A physical volume measured in milliliters.

### 1.3 Referenced Publications

*European Journal of Nuclear Medicine* vol. 18, no. 6, 1991. Bailey DL, Jones T, and Spinks TJ. "A Method for Measuring the Absolute Sensitivity of Positron Emission Tomographic Scanners," pp. 374-379.

*Journal of Nuclear Medicine*, vol. 43, no. 10, 2002. Daube-Witherspoon ME, Karp JS, Casey ME, DiFilippo FP, Hines H, Muehllehner G, Simcic V, Stearns CW, Adam L-E, Kohlmyer S and Sossi V. "PET Performance Measurements Using the NEMA NU 2-2001 Standard," pp. 1398-1409.

*Journal of Nuclear Medicine*, vol. 28, no. 11, 1987. Daube-Witherspoon ME and Muehllehner G. "Treatment of axial data in three-dimensional PET." pp. 1717-1724.

*IEEE Transactions on Nuclear Science*, vol. 37, no. 2, 1990. Strother SC, Casey ME, and Hoffman EJ. "Measuring PET Scanner Sensitivity: Relating Countrates to Image Signal-to-Noise Ratios using Noise Equivalents Counts." pp. 783-788.

*Journal of Nuclear Medicine*, vol. 45, no. 5, 2004. Watson CC, Casey ME, Eriksson L, Mulnix T, Adams D and Bendriem B. "NEMA NU 2 Performance Tests for Scanners with Intrinsic Radioactivity." pp. 822-826.

*IEEE Transactions on Nuclear Science*, vol. 63, no. 3, 2016. Wang G-C, Li X, Niu X, Du H, Balakrishnan K, Ye H, and Burr K, "PET Timing Performance Measurement Method Using NEMA NEC Phantom," pp. 1335-1342.

*NIST Standard Reference Database 120: Radionuclide Half-life Measurements*. [Online]  
<http://www.nist.gov/pml/data/halflife.cfm>. Accessed 10 August 2017.

*NEMA PS3 / ISO 12052, Digital Imaging and Communications in Medicine (DICOM) Standard*, National Electrical Manufacturers Association, Rosslyn, VA, USA (available free at <http://medical.nema.org/>).

## Section 2 General

### 2.1 Purpose

The intent of this standards publication is to specify procedures for evaluating performance of positron emission tomographs. The resulting standardized measurements can be cited by manufacturers to specify the guaranteed performance levels of their tomographs. As these measures become available throughout the industry, potential customers may compare the performance of tomographs from various manufacturers. The standard measurement procedures can be used by customers for acceptance-testing of tomographs before and after installation of the equipment.

In defining this standard, language referring to levels of a standard such as "class standard" versus "performance standard" or "typical values" versus "meet or exceed" has been avoided. Determining the frequency of sampling of systems for each test is left to the manufacturer. Because both the difficulty of performing the various measurements and the accuracy of each test's results vary, the decision of quoting a result as a typical or met/exceeded value is also left to the manufacturer.

### 2.2 Purview

It is assumed that every system to be tested under this standard is able to create sinograms and transverse slice images, define and manipulate two-dimensional regions of interest with circular and rectangular boundaries, and extract such parameters as coincidence event counts detected within specified intervals of time. The system is also assumed to have transverse fields of view suitable for human subjects. For all of the procedures, except for the image quality test, the scanner must have an accessible diameter of at least 260 millimeters. The test phantom for all of the procedures, except for the image quality test, is 70.0 cm in length and is suitable for performing measurements in all slices of tomographs with an axial field of view of less than 65 cm. The image quality test, which requires a different test phantom, can only be performed on a scanner with an accessible diameter of at least 350 millimeters. While this precludes the performance of the image quality test on some brain-only scanners, it is important to note that the image quality test is designed to emulate whole-body imaging performance, and therefore is not appropriate for a brain-only tomograph.

The intent of this standard is to provide a set of measurements that permit the comparison of positron emission tomograph performance. Though it may be useful to have tests tailored to specific tasks or patient geometries, such additional tests do not add substantial value to the comparison of systems. The range of tests in this standard is not intended to restrict or discourage alternative tests.

A specific example would be the NU 2-1994 scatter fraction and count rate test. The source geometry in this test is a better approximation to the human brain than the 70 cm source length in the current standard. However, for the purposes of general comparison, a system that performs better on the method in this standard will also be better on the geometry-specific test. A comprehensive comparison in different geometries is a valid topic for the research literature but is not suitable for a test standard that may be applied to a production environment.

The measurements described in this standards publication have been designed with a primary focus on whole-body imaging for oncologic applications. As such, these measurements may not accurately represent the performance of a positron emission tomograph in brain imaging applications. These specifications represent a subset of measurements that define the performance of positron emission tomographs.

### 2.3 Units of Measure

Système International d'Unités (SI) units shall be used in all reports of positron emission tomograph performance measurements. Customary units such as millicuries may be optionally reported as auxiliary values in parenthetical statements with the standard specifications for individual performance reports.

### 2.4 Consistency

All measurements must be performed without altering any of the instrument's parameters that are mutually exclusive unless otherwise directed for a particular measurement. These include, but are not limited to, the following parameters: energy discrimination windows (including the utilization of multiple energy windows in photopeak-Compton imaging modes), coincidence timing window(s), pulse integration time, reconstruction algorithm with associated parameters, pixel size, slice thickness, axial acceptance angle, and axial averaging or smoothing. If multiple operating modes are supported by the instrument, the operating mode used for each measurement shall be clearly specified.

For instruments with movable detector elements, the detector positions and trajectories shall be those recommended by the manufacturer and shall remain the same for all acquisitions. These motions include but are not limited to, the detector separation distance, orbit trajectory around the patient to produce a full tomographic data set, and motions to increase sampling such as detector wobble or table displacements. The reconstruction algorithm, with its associated parameters, matrix, and pixel size shall be that recommended by the manufacturer and shall remain fixed for all of the NEMA measurements of tomograph performance unless otherwise directed for a particular measurement.

Most systems organize the raw measurements into parallel projection matrices corresponding to transverse slices before performing a 2-D tomographic image reconstruction. This can lead to errors in positioning depending on the axial acceptance angle, particularly in the axial direction, as the radial distance from the center increases. Some systems can change the axial acceptance angle by adjusting the septa shielding, while others specify the angle in software. For systems that acquire and reconstruct 3-D measurements, it is assumed that the volume imaged can be oriented into transaxial slices for data analysis. The acceptance angle shall be that recommended by the manufacturer and shall remain fixed for all of the NEMA measurements of tomograph performance.

Some measurements explicitly require volumetric data to be re-sorted into transverse sinograms using the single-slice rebinning method, as described in Daube-Witherspoon, M.E. and Muehllehner, G., "Treatment of axial data in three-dimensional PET," *Journal of Nuclear Medicine* 28:1717-1724, 1987, for all other measurements, the manufacturer's recommended treatment of volumetric data shall be used.

The energy window or windows used for these measurements must be specified. If multiple windows are used in a photopeak-Compton imaging mode, that mode shall also be specified. These window settings shall be those recommended by the manufacturer and shall remain fixed during all of the NEMA measurements of a tomograph's performance.

Each measurement procedure specifies the method of source support, whether the source is to be suspended in the field of view or supported by some means. For those measurements in which the source is to be supported, the source shall be placed on the patient table.

Unless specified otherwise in the description of a particular measurement, phantom positioning instructions carry a nominal tolerance of 5 mm in both the transaxial and the axial directions.

### 2.5 Equivalency

<sup>18</sup>F is specified for all of the tests, with the exception that <sup>22</sup>Na may be used in the spatial resolution test in Section 3 and the PET/CT coregistration accuracy test in Section 9. For some measurements, substitution of another radionuclide, such as <sup>68</sup>Ga, can lead to significantly different results due to such factors as positron range and activity calibration. If for quality assurance or other purposes, a

manufacturer employs measurement methods other than those prescribed, the manufacturer shall demonstrate traceability between the methods prescribed for the measurement and those employed for testing.

It is assumed that the dose calibrator or well counter used for these measurements has been calibrated using either a National Institute of Standards and Technology reference source or one whose activity has been closely related or traceable to a reference source.

## Section 3 Spatial Resolution

### 3.1 General

The spatial resolution of a system represents its ability to distinguish between two points after image reconstruction. The measurement is performed by imaging point sources in air and then reconstructing images with no smoothing or apodization. Although this does not represent the condition of imaging a subject in which tissue scatter and a limited number of acquired events require the use of a smooth reconstruction filter, the measured spatial resolution provides a best-case comparison among scanners, indicating the highest achievable performance.

### 3.2 Purpose

The purpose of this measurement is to characterize the widths of the reconstructed image point spread functions (PSF) of compact radioactive sources. The width of the point spread function is measured by its full width at half-maximum amplitude (FWHM) and full width at tenth-maximum amplitude (FWTM).

This measurement method characterizes the intrinsic spatial resolution of the data produced by the scanner. It does not characterize the reconstruction process or spatial resolution of a clinical image

### 3.3 Method

For all systems, the spatial resolution shall be measured in the transverse slice in two directions (e.g., radially and tangentially). In addition, an axial resolution also shall be measured.

The transverse field of view and image matrix size determine the pixel size in the transverse slice. In order to measure the width of the point spread function as accurately as can practically be achieved, its FWHM should span at least three pixels. The pixel size should be made no more than one-third of the expected FWHM in all three dimensions during reconstruction and should be reported for the spatial resolution measurement.

#### 3.3.1 Radionuclide

The radionuclide for this measurement shall be  $^{18}\text{F}$  or  $^{22}\text{Na}$ , with an activity sufficiently low that at least one of the following is true:

- a. the percent dead time losses are less than five percent, or
- b. the random coincidence rate is less than five percent of the total event rate.

#### 3.3.2 Source Distribution

The point sources shall each consist of a small quantity of concentrated activity of less than or equal to 1 mm in each direction. A capillary tube or other object may be used to enclose the activity.

The sources shall be located at six points as follows:

- a. In the axial direction, along planes at the center of the axial FOV and three-eighths of the axial FOV from the center of the FOV (i.e., one-eighth of the axial FOV from the end of the tomograph).
- b. In the transverse direction, the source shall be positioned at 1 cm (to represent the center of the FOV, but positioned to avoid any possible inconsistent results at the very center of the FOV), 10 cm, and 20 cm from the center of the plane (the 20 cm location shall be omitted if it is not covered by the transverse field of view). The sources shall be positioned on either the horizontal

or vertical line intersecting the system axis so that the radial and tangential directions are aligned with the image grid. The positioning accuracy in the transaxial plane shall be  $\pm 2$  mm for the source at 1 cm offset, and  $\pm 5$  mm for the sources at offsets of 10 cm and 20 cm. The positioning accuracy in the axial direction shall be  $\pm 2$  mm for all sources.

### 3.3.3 Data Collection

Measurements shall be collected at all six positions specified above. At least one hundred thousand counts shall be acquired in each response function. Measurements can be taken with multiple sources. Finer sample size may be selected than typically used in clinical studies.

### 3.3.4 Data Processing

Reconstruction by filtered back projection with no smoothing or apodization shall be employed for all spatial resolution data.

Results obtained using alternate reconstruction algorithms may be reported in addition to the filtered back projection results, provided that the alternate reconstruction methods and their parameters are described in sufficient detail to reproduce the study results.

## 3.4 Analysis

The spatial resolution (FWHM and FWTM) of the point source response function in all three directions shall be determined by forming one-dimensional response functions, along profiles through the image volume in three orthogonal directions, through the peak of the distribution. The width of the response functions in the two directions at right angles to the direction of measurement shall be approximately two times the FWHM.

Each FWHM (and FWTM) shall be determined by linear interpolation between adjacent pixels at half (or one-tenth) the maximum value of the response function (see Figure 3-1). The maximum value shall be

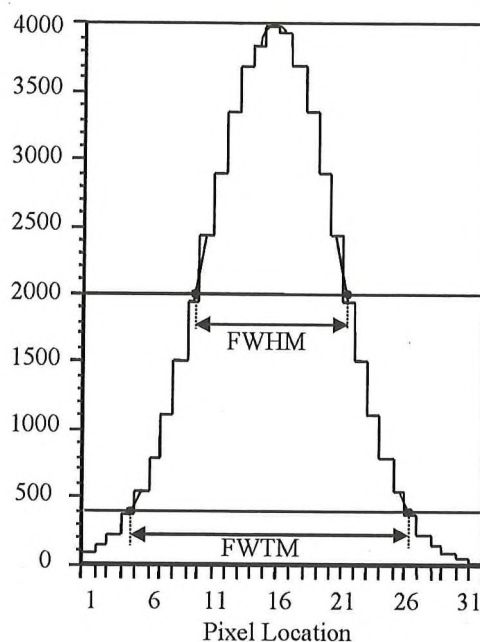


**Figure 3-1**  
**A Typical Response Function with FWHM and FWTM Determined Graphically by Interpolation**

determined by a parabolic fit using the peak point and its two nearest neighboring points respectively. Values shall be converted to distance in millimeters by multiplication by the pixel size.

The observed source location shall be determined as the location of the pixel containing the maximum number of counts in each one-dimensional response function.

### **3.5 Report**

Report the source nuclide and dimensions.

Axial, radial and tangential resolutions (FWHM and FWTM) for each radius (1, 10 and 20 cm), averaged over both axial positions, shall be calculated and reported as values of system resolution.

If alternate reconstruction methods were used, the results of the tests should be reported together with the exact description of the methodology.

The observed source location is to be reported individually for each source to allow verification of correct positioning per Section 3.3.2.

## Section 4 Scatter Fraction, Count Losses, and Randoms

### 4.1 General

The scattering of gamma rays emitted by the annihilation of positrons results in falsely located coincidence events. Variations in design and implementation cause positron emission tomographs to have different sensitivities to scattered radiation.

The measurements of count losses and random rates express the ability of a positron emission tomograph to measure highly radioactive sources.

Two methods are described for the analysis and reporting of this measurement. The first method requires the measurement of random coincidences, whether by a delayed event channel or a calculation from single-detector event rates. This method is preferred, since it allows the estimation of scatter fraction as a function of count rate, and it is required for instruments with an intrinsic background that are unable to achieve a randoms-to-true ratio of less than one percent. The second method is an alternate method available for those systems that lack a randoms measurement capability.

The measurement of noise equivalent count rates is based on work described in Strother, S.C., Casey, M.E., and Hoffman, E.J., "Measuring PET Scanner Sensitivity: Relating Count-Rates to Image Signal-to-Noise Ratios Using Noise Equivalent Counts," *IEEE Transactions on Nuclear Science* NS-37(2):783-788, 1990. The adaptation of these methods to scanners with intrinsic background counts is discussed in Watson, C.C. et al., "NEMA NU 2 Performance Tests for Scanners with Intrinsic Radioactivity," *Journal of Nuclear Medicine*, 45(5):822-826, 2004.

### 4.2 Purpose

The first purpose of this procedure is to measure the relative system sensitivity to scattered radiation. Scatter is expressed by the scatter fraction, SF, for the entire tomograph. The second purpose of this procedure is to measure the effects of system dead time and the generation of random events at several levels of source activity. The true event rate is the total coincident event rate minus the scattered event rate and minus the randoms event rate.

### 4.3 Method

The test phantom is a solid right circular cylinder composed of polyethylene with a specific gravity of  $0.96 \pm 0.01$ , with an outside diameter of  $203 \pm 3$  mm (8" nom.), and with an overall length of  $700 \pm 5$  mm. A  $6.4 \pm 0.2$  mm (1/4" nom.) hole is drilled parallel to the central axis of the cylinder, at a radial distance of  $45 \pm 1$  mm. For ease of fabrication and handling, the cylinder may consist of several segments that are assembled together during testing. However, in both design and assembly of the completed phantom, one must insure a tight fit between adjacent segments, as even very small gaps will allow narrow axial regions of scatter-free radiation.

The test phantom line source insert is a clear polyethylene or polyethylene coated plastic tube at least 800 mm in length, with an inside diameter of  $3.2 \pm 0.2$  mm (1/8" nom.) and an outside diameter of  $4.8 \pm 0.2$  mm (3/16" nom.). The central  $700 \pm 20$  mm of this tube will be filled with a known quantity of activity and threaded through the 6.4 mm hole in the test phantom.

To begin the test, a source of relatively high activity is placed in the field of view of the positron emission tomograph. Regular measurements are then taken while the activity in the phantom decays over several half-lives. A decrease in the event rate accompanies the activity decay.

In addition, the efficiency of the system in processing coincident events improves as the activity decays, until count losses may be effectively neglected. Thus, by waiting long enough, one obtains a measurement of the coincidence count rate that is effectively free from processing losses. By extrapolating this true rate back to higher activity levels and comparing it to the measured rate one may estimate count losses suffered by the system at higher activity levels. The accuracy of this technique depends critically on adequate statistics being gathered at sufficiently low levels of activity. This may require repeated measurements at the lower count rates.

#### 4.3.1 Symbols

**Scatter fraction (SF)**—a dimensionless ratio of scattered coincidence events to the sum of scattered and true coincidence events in a defined region of interest (ROI) in the scanner's field of view.

#### 4.3.2 Radionuclide

The radionuclide used for this measurement shall be  $^{18}\text{F}$ . The amount of radioactivity shall be great enough to allow the following two rates to be measured:

- a.  $R_{t,\text{peak}}$  – peak true count rate
- b.  $R_{\text{NEC},\text{peak}}$  – peak noise equivalent count rate

Recommendations for the initial activity required to meet these objectives will be supplied by the manufacturer.

The initial activity in the phantom,  $A_{\text{cal,meas}}$ , shall be determined from the activity injected into the phantom as measured in a calibrated dose calibrator. The central  $700 \pm 20$  mm of the test phantom line source insert shall be filled with water well mixed with the measured amount of radioactivity and sealed at both ends. There should be no significant void regions (bubbles) within the active length of the source.

In order to account for possible variations in source length, the length of the water-filled region shall be measured after filling. The corrected initial activity,  $A_{\text{cal}}$ , shall be computed as:

$$A_{\text{cal}} = A_{\text{cal,meas}} \frac{700\text{mm}}{L_{\text{meas}}}$$

where  $A_{\text{cal,meas}}$  is the measured activity and  $L_{\text{meas}}$  is the measured source length in millimeters. This corrected initial activity shall be used for the analysis below, as well as for the analyses performed in Section 6.

#### 4.3.3 Source Distribution

The line source shall be inserted into the hole of the test phantom such that the region of activity is centered with respect to the 70 cm length of the phantom. The test phantom with line source is mounted on the standard patient table supplied by the manufacturer and rotated such that the line source insert is positioned nearest to the patient table (see Figure 4-1). The phantom is placed parallel to the scanner's axis and centered in the transverse and axial fields-of-view to within 5 mm.

To obtain accurate results, the test phantom must be centered in the FOV, and the table shall be positioned such that the trough of the table is positioned  $15 \pm 1$  cm below the center of the transverse FOV (equivalent to centering a patient in the center of the transverse FOV). Foam blocks or similar devices positioned axially outside the FOV of the scanner shall be used to support the phantom and elevate it above the trough of the table.

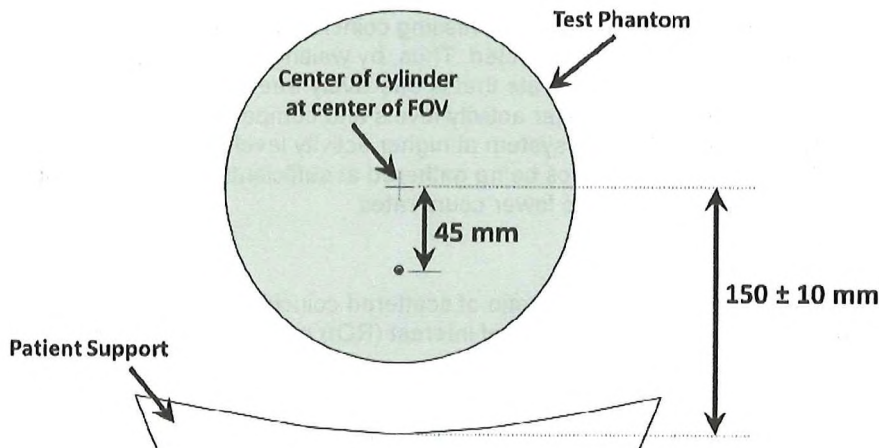


**Figure 4-1**  
**Positioning of Phantom**

Although some scanners may optionally employ equipment other than the patient table within the FOV for certain scans, e.g., pads or cushions, or local RF coils for PET/MR systems, only permanent fixtures used routinely for clinical scans must be present in the FOV for this test.

#### 4.3.4 Data Collection

Data shall be acquired at intervals more frequent than half the radionuclide half-life,  $T_{1/2}$ , until true events losses are less than 1.0%. If the data will be processed with the alternate (no randoms measurement) method, data shall be acquired so that the true event losses are less than 1.0% and the randoms-to-true ratio is also less than 1.0% for the final three frames of the acquisition sequence. The durations of the individual acquisitions,  $T_{\text{acq},j}$ , shall be less than one-fourth of  $T_{1/2}$ . Acquisitions shall be fully tomographic; therefore, rotating scanners must rotate to provide complete and uniform angular sampling for each acquisition. In the case of rotating scanners, the acquisition time  $T_{\text{acq}}$  shall include the time required to rotate the detectors.

If a randoms estimate is available, the number of random counts,  $C_{r,i,j}$  for each acquisition,  $j$ , and each slice,  $i$ , shall be recorded. The method of 4.4.1 shall be employed to find the random event rate. If randoms estimation is not available, the method of 4.4.2 shall be employed. The report shall specify if a randoms estimate was used, and, if so, which method of randoms estimation was used.

If time-of-flight measurement is available, the TOF information may be recorded in the acquired data, for example, sinogram or list mode. The TOF information is required for these data to be used for the time-of-flight resolution measurement in Section 8.

Each acquisition should contain a minimum of 500,000 prompt counts. It is also important that the measurements around the peak count rate be done with sufficient frequency so that the peak rate can be accurately determined. Therefore, it is expected that manufacturers will recommend a protocol for their scanners that includes starting activity, acquisition times, and acquisition durations.

#### 4.3.5 Data Processing

For tomographs with an axial field of view of 65 cm or less, prompt and random sinograms shall be generated for each acquisition  $j$  of slice  $i$ . (If no randoms estimate is available, only prompt sinograms are generated.) For tomographs with an axial field of view greater than 65 cm, sinograms shall be generated for each acquisition for slices within the central 65 cm. No corrections for variations in detector sensitivity

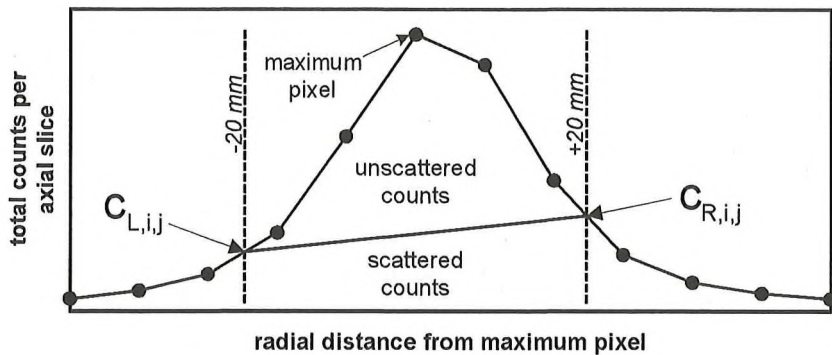


**Figure 4-2**  
**Integration of Background Counts Inside and Outside 40-mm Strip**

or detector motions such as wobble, randoms, scatter, dead time, or attenuation shall be applied to the measurements.

Oblique sinograms are collapsed into a single sinogram for each respective slice (by single-slice rebinning) while conserving the number of counts in the sinogram. If the relation between radial sinogram pixel (bin) number and radial distance is the same for all slices, then the analysis below may be further simplified by summing all the sinograms together to form a single slice and processing only this single slice. In this case, it is important to note that accurate results depend on having the line source parallel to the scanner's axis.

#### 4.4 Analysis

Each prompt sinogram  $i$  of each acquisition  $j$  is processed as follows:

- All pixels located farther than 12 cm from the center of the scanner's transaxial field of view shall be set to zero. The radial position of a pixel is defined as the radial offset of the mean physical line-of-response measured by the pixel.
- For each projection angle  $\phi$  within the sinogram, the location of the center of the line source response shall be determined either by finding the pixel having the greatest value, or by estimating this location using an interpolation or fitting technique. The latter may be preferred for sinograms containing gaps (unmeasured pixels). The technique used for determining the center location shall be reported.
- Each projection shall be shifted so that the pixel at the center of the line source response is aligned with the central pixel of the sinogram.
- After alignment, a sum projection shall be produced by summing this aligned sinogram over projection angle. In other words, the counts in a pixel in the sum projection is the sum of the counts in the pixels in each angular projection having the same radial pixel offset from the center of the line source response as the pixel in the sum projection has from the center of the sinogram:

$$C(r)_{i,j} = \sum_{\phi} C(r - r_{\text{center}}(\phi), \phi)_{i,j}$$

where:

- $r$  is the pixel number in a projection, with  $r = 0$  being the radial center of the sinogram;
- $\phi$  is the projection number in the sinogram (i.e., the sinogram row);
- $r_{\text{center}}(\phi)$  refers to the center of the line source response in projection  $\phi$ .

- e. The counts per pixel,  $C_{L,i,j}$  and  $C_{R,i,j}$ , at the left and right edges, respectively, of the 40 mm wide strip at the center of the sinogram, shall be obtained from the sum projection using linear interpolation (see Figure 4-2). The interpolation points should correspond to physical distances of  $\pm 20$  mm from the center of a normal (un-shifted) sinogram. The interpolating line for  $C_{L,i,j}$  ( $C_{R,i,j}$ ) is to be drawn between the center points of the two pixels nearest to  $C_{L,i,j}$  ( $C_{R,i,j}$ ), using their measured values (counts per pixel) at these points.
- f. The average of the two interpolated pixel intensities  $C_{L,i,j}$  and  $C_{R,i,j}$  shall be multiplied by the number of pixels, including fractional values, between the edges of the 40 mm wide strip, and the product added to the integral of the counts in the pixels outside the strip, including partial pixels, to yield the number of random plus scatter counts  $C_{r+s,i,j}$  for the slice  $i$  of acquisition  $j$ . The integral of the counts in the partial pixels adjacent to  $C_{L,i,j}$  and  $C_{R,i,j}$  outside the strip shall be based on the same interpolation lines used for estimating  $C_{L,i,j}$  and  $C_{R,i,j}$ .
- g. The total event counts  $C_{TOT,i,j}$  are computed as the sum of all pixels in the sum projection for slice  $i$  of acquisition  $j$ .

The average activity  $A_{ave,j}$  for each acquisition  $j$  shall be calculated (see Section 1.2).

Subsequent analysis is dependent on whether or not a randoms estimate is available:

#### 4.4.1 Analysis with Randoms Estimate

All pixels in each randoms sinogram  $i$  of acquisition  $j$  located farther than 12 cm from the center of the scanner's transaxial field of view shall be set to zero. The number of randoms counts,  $C_{r,i,j}$ , is found by summing the remaining counts in sinogram  $i$ , of acquisition  $j$ .

##### 4.4.1.1 Scatter Fraction

The system scatter fraction of acquisition  $j$ ,  $SF_j$ , is computed by summing the counts over slices as follows:

$$SF_j = \frac{\sum_i C_{r+s,i,j} - \sum_i C_{r,i,j}}{\sum_i C_{TOT,i,j} - \sum_i C_{r,i,j}}$$

##### 4.4.1.2 Count Rates and NECR

For each acquisition  $j$ , compute the system event rates:

- a. The total event rate  $R_{TOT,j}$ :

$$R_{TOT,j} = \frac{1}{T_{acq,j}} \sum_i C_{TOT,i,j}$$

- b. the true event rate  $R_{t,j}$ :

$$R_{t,j} = \frac{1}{T_{acq,j}} \sum_i (C_{TOT,i,j} - C_{r+s,i,j})$$

- c. the random event rate  $R_{r,j}$ :

$$R_{r,j} = \frac{1}{T_{acq,j}} \sum_i C_{r,i,j}$$

- d. and the scatter event rate  $R_{s,j}$ :

$$R_{s,j} = \frac{1}{T_{acq,j}} \sum_i (C_{r+s,i,j} - C_{r,i,j})$$

where  $T_{\text{acq},j}$  is the acquisition time for frame  $j$ .

Systems that use an unprocessed delayed channel for randoms estimation shall compute  $R_{\text{NEC},j}$  for each acquisition  $j$  as:

$$R_{\text{NEC},j} = \frac{R_{t,j}^2}{R_{\text{TOT},j} + R_{r,j}}$$

All other systems, including those using a processed, delayed channel or a singles-event based randoms estimator, shall compute the noise equivalent count rate  $R_{\text{NEC},j}$  for each acquisition  $j$  as:

$$R_{\text{NEC},j} = \frac{R_{t,j}^2}{R_{\text{TOT},j}}$$

#### 4.4.2 Alternative Analysis with No Randoms Estimate

##### 4.4.2.1 Scatter Fraction

The final three acquisitions  $j'$  of the sequence with count loss rates and random rates below 1.0% of the true rate shall be used to determine the scatter fraction. For these acquisitions, it is assumed that  $C_{r+s,i,j'}$  has a negligible number of random counts and consists only of scatter counts, and likewise,  $C_{\text{TOT},i,j'}$  consists only of true and scatter counts.

The system scatter fraction  $SF$  is computed as follows:

$$SF = \frac{\sum_i \sum_{j'} C_{r+s,i,j'}}{\sum_i \sum_{j'} C_{\text{TOT},i,j'}}$$

##### 4.4.2.2 Count Rates and NECR

For each acquisition  $j$ , compute the system event rates:

e. The total event rate  $R_{\text{TOT},j}$ :

$$R_{\text{TOT},j} = \frac{1}{T_{\text{acq},j}} \sum_i C_{\text{TOT},i,j}$$

f. the true event rate  $R_{t,j}$ :

$$R_{t,j} = \frac{1}{T_{\text{acq},j}} \sum_i (C_{\text{TOT},i,j} - C_{r+s,i,j})$$

g. the random event rate  $R_{r,j}$ :

$$R_{r,j} = R_{\text{TOT},j} - \left( \frac{R_{t,j}}{1 - SF} \right)$$

h. and the scatter event rate  $R_{s,j}$ :

$$R_{s,j} = \left( \frac{SF}{1 - SF} \right) R_{t,j}$$

where  $T_{\text{acq},j}$  is the acquisition time for frame  $j$ .

Systems that use an unprocessed delayed channel for randoms estimation shall compute  $R_{NEC,j}$  for each acquisition  $j$  as:

$$R_{NEC,j} = \frac{R_{t,j}^2}{R_{TOT,j} + R_{r,j}}$$

All other systems, including those using a processed, delayed channel or a singles-event based randoms estimator, shall compute the noise equivalent count rate  $R_{NEC,j}$  for each acquisition  $j$  as:

$$R_{NEC,j} = \frac{R_{t,j}^2}{R_{TOT,j}}$$

## 4.5 Report

### 4.5.1 Count Rate Plot

For the system, plot the following five quantities as a function of the average effective radioactivity concentration  $a_{ave,j}$ , as defined in Section 1.2, where the volume  $V$  is the total volume of the cylindrical phantom (22,000 mL):

- a.  $R_{t,j}$  – system true event rate
- b.  $R_{r,j}$  – system random event rate
- c.  $R_{s,j}$  – system scatter event rate
- d.  $R_{NEC,j}$  – system noise equivalent count rate
- e.  $R_{TOT,j}$  – system total event rate

Also report the method used for estimating randoms, if one was used in the measurement.

### 4.5.2 Peak Count Values

Report the following values, derived from the above plot:

- a.  $R_{t,peak}$  – peak true count rate
- b.  $R_{NEC,peak}$  – peak noise equivalent count rate
- c.  $a_{t,peak}$  – the activity concentration at which  $R_{t,peak}$  is reached
- d.  $a_{NEC,peak}$  – the activity concentration at which  $R_{NEC,peak}$  is reached

### 4.5.3 System Scatter Fraction

If a randoms estimate was used in the measurement, report the value of  $SF$  at peak noise equivalent count rate and plot system scatter fraction  $SF_j$  versus activity  $a_{ave,j}$  as defined in Section 4.5.1.

If no randoms estimate was used in the measurement, report the value  $SF$ .

### 4.5.4 Table and Phantom Positioning, and Projection Alignment

Confirm that the patient handling system is positioned such that the trough of the table is positioned  $15 \pm 1$  cm below the center of the transverse FOV.

## Section 5 Sensitivity

### 5.1 General

Sensitivity of a positron emission tomograph is expressed as the rate in counts per second that true coincidence events are detected for a given source strength. Since the emitted positrons annihilate and create a pair of gamma rays, a significant amount of material must surround the source to insure annihilation. This surrounding material also attenuates the created gamma rays, prohibiting a measurement without interfering attenuation. To arrive at an attenuation free measurement, successive measurements are made with a uniform line source surrounded by known absorbers. From these measurements, the sensitivity with no absorber can be extrapolated.

This measurement technique is based on work described in Bailey, D.L., Jones, T., and Spinks, T.J., "A Method for Measuring the Absolute Sensitivity of Positron Emission Tomographic Scanners," *European Journal of Nuclear Medicine* 18: 374-379, 1991.

### 5.2 Purpose

The purpose of this procedure is to measure the sensitivity or ability of the scanner to detect positrons.

### 5.3 Method

The test equipment required for this measurement is the sensitivity phantom shown in Figure 5-1.

#### 5.3.1 Symbols

**Accumulated Sleeve Wall Thickness ( $X$ )** – the combined thickness of the metal sleeve walls used in the sensitivity measurement.

**Attenuation Coefficient ( $\mu$ )** – a measure of the likelihood that a photon will undergo an interaction while traveling through a material, expressed in units of reciprocal distance (such as  $\text{mm}^{-1}$ ).

**Sensitivity ( $S$ )** – a measure of the rate at which coincidence events are detected in the presence of radioactive sources in the limit of low activity levels where count rate losses are negligible.

- a.  $S_i$  – sensitivity of slice  $i$
- b.  $S_{\text{tot}}$  – total system sensitivity

#### 5.3.2 Radionuclide

The radionuclide for this measurement shall be  $^{18}\text{F}$ , with an activity sufficiently low that at least one of the following is true:

- a. the percent dead time losses are less than 5%, or,
- b. the random coincidence rate is less than 5% of the total event rate.

For systems that provide measurement of the randoms rate, the randoms rate may be subtracted, and the trues only sensitivity can then be reported. For systems with intrinsic randoms, those randoms-subtracted value must be reported.

The initial activity in the phantom shall be determined by measurement in a dose calibrator.

### 5.3.3 Source Distribution

A  $700 \pm 20$  mm portion of plastic tubing shall be filled with water, well mixed with a measured amount of radioactivity, and sealed at both ends. This activity,  $A_{\text{cal,meas}}$  in MBq, and the time of the assay,  $T_{\text{cal}}$ , should be recorded. The phantom is suspended in the center of the transaxial field of view, aligned with the axis of the tomograph in such a way that any supporting mechanism is external to the field of view. Ensure that the center of the phantom is centered in the axial field of the tomograph.

In order to account for possible variations in source length, the length of the water-filled region shall be measured after filling. The corrected initial activity,  $A_{\text{cal}}$ , shall be computed as:

$$A_{\text{cal}} = A_{\text{cal,meas}} \frac{700 \text{ mm}}{L_{\text{meas}}}$$

where  $A_{\text{cal,meas}}$  is the measured activity and  $L_{\text{meas}}$  is the measured source length in millimeters. This corrected initial activity shall be used for the analysis below.

### 5.3.4 Data Collection

Data are collected for a period of time to ensure that at least 10,000 trues per slice are collected. Single slice rebinning shall be used to assign counts in oblique lines-of-response (LORs) to the image slice where the LOR crosses the scanner axis. The starting time of the measurement,  $T_j$ , is recorded along with the duration,  $T_{j,\text{acq}}$ , and the number of counts collected. In the case of scanners whose detectors must be moved to acquire a full tomographic data set, the acquisition time  $T_{j,\text{acq}}$  shall include the time required to move the detectors. The rate,  $R_{j,i}$ , in counts per second, shall be determined by dividing the counts collected in the slice by the duration. In succession, each of the four sleeves is added to the phantom and the measurement repeated, recording values for  $T_j$  and  $R_{j,i}$  for each measurement. The test may also be performed starting with all sleeves in place and successively removing the outermost one.

If applicable, the randoms rate for each measurement is to be recorded separately. This value is to be subtracted prior to the calculations in Section 5.4.

To assess the sensitivity at different radial positions, the process described in the preceding paragraph shall be repeated at a 10 cm radial offset from the center of the transaxial field of view.

## 5.4 Calculations and Analysis

### 5.4.1 System Sensitivity

For each measurement associated with each of the five sleeves, calculate the total count rate  $R_j$  by summing the  $R_{j,i}$  from each slice  $i$ . Correct each count rate  $R_j$  for radioactive decay by the following formula:

$$R_{\text{CORR},j} = \frac{(T_{j,\text{acq}} \ln 2) \exp\left(\frac{T_j - T_{\text{cal}}}{T_{1/2}} \ln 2\right)}{T_{1/2} \left[1 - \exp\left(-\frac{T_{j,\text{acq}}}{T_{1/2}} \ln 2\right)\right]} R_j .$$

Fit the data to the following equation using regression:

$$R_{\text{CORR},j} = R_{\text{CORR},0} \times \exp(-\mu_M \cdot 2X_j) ,$$

where  $R_{\text{CORR},j}$  and  $\mu_M$  are the unknowns, and  $X_j$  represents the accumulated sleeve wall thickness. The term  $R_{\text{CORR},0}$  represents the count rate with no attenuation. The value for attenuation in metal,  $\mu_M$ , is allowed to vary to compensate for the small amount of scattered radiation.

The same procedure shall be followed for the sensitivity measurements done at 10 cm offset from the tomograph center.

The system sensitivity shall be computed by the following formula.

$$S_{\text{tot}} = \frac{R_{\text{CORR},0}}{A_{\text{cal}}}$$

#### 5.4.2 Axial Sensitivity Profile

Using the data collected for the smallest tube,  $R_{1,i}$ , at the 0 centimeter radial offset, compute the sensitivity for each slice by the following:

$$S_i = \frac{R_{1,i}}{R_1} \cdot S_{\text{tot}}$$

#### 5.5 Report

Report the sensitivity for each of the radial offsets in counts/sec/kBq. Also, report the axial sensitivity profile by plotting the sensitivity,  $S_i$ , for each slice. Specify if reported values are calculated after the subtraction of randoms or, if unable to correct for randoms, with an acquired randoms fraction of less than five percent.

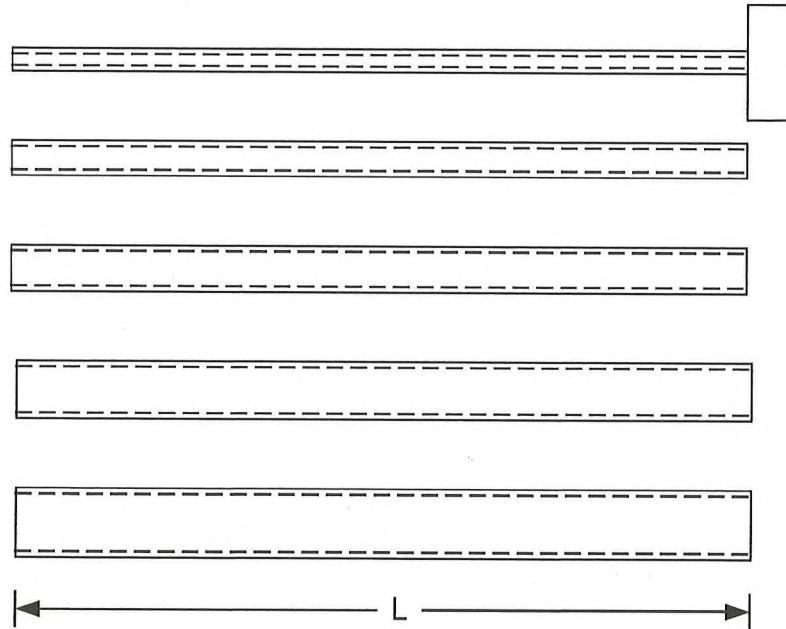


**Figure 5-1**  
**Sensitivity Measurement Phantom (Not to Scale)**

| Sleeve Number | Inside Diameter (mm) | Outside Diameter (mm) | Length L (mm) |
|---------------|----------------------|-----------------------|---------------|
| 1             | 3.9                  | 6.4                   | 700           |
| 2             | 7.0                  | 9.5                   | 700           |
| 3             | 10.2                 | 12.7                  | 700           |
| 4             | 13.4                 | 15.9                  | 700           |
| 5             | 16.6                 | 19.1                  | 700           |

## Section 6

### Accuracy: Corrections for Count Losses and Randoms

#### 6.1 General

To achieve quantitative measurements of source activity distributions under widely varying conditions, positron emission tomographs usually can compensate for dead time losses and random events. The accuracy of these corrections, particularly at the highest count rates encountered in clinical imaging, is reflected by the bias with which the tomograph reports counts. The following test uses a simple activity distribution and is not representative of a wide variety of imaging conditions. However, such a test would require a considerable amount of time to perform and require handling large amounts of radioactivity.

#### 6.2 Purpose

The purpose of this procedure is to measure the accuracy of corrections for dead time losses, and random event counts in images.

#### 6.3 Method

The test phantom data of Section 4.3, acquired for measurements of random rates and dead time losses, shall be used to measure the net error in count rate after correction for dead time losses and randoms.

##### 6.3.1 Symbols

**Relative count rate error ( $\Delta r$ ):** the difference between the expected count rate and the measured count rate, expressed as a percentage of the expected rate.

##### 6.3.2 Radionuclide

The radionuclide used for this measurement shall be  $^{18}\text{F}$ . See Section 4.3.2 for information regarding the amount of activity to be used for this test.

##### 6.3.3 Source Distribution

See Section 4.3.3 for a description of the source distribution for this test.

##### 6.3.4 Data Collection

See Section 4.3.4 for a description of the acquisition parameters for this test.

##### 6.3.5 Data Processing

For tomographs with an axial field of view of 65 cm or less, all slices shall be reconstructed. For tomographs with an axial field of view greater than 65 cm, only slices in the central 65 cm shall be reconstructed. Attenuation, scatter, randoms and dead time corrections shall be applied to the data, using the most accurate available means. Decay correction shall not be applied to the data. Images shall be reconstructed using the standard whole-body algorithm. These methods shall be reported.

#### 6.4 Analysis

All analyses shall be performed on each reconstructed image  $i$  of each acquisition  $j$ . Image slices outside of the central 80% of the axial field of view shall be excluded from the analysis. The average activity  $A_{\text{ave},j}$  for each acquisition  $j$  shall be calculated (see Section 1.2). The average effective activity concentration  $a_{\text{eff},j}$  for each acquisition  $j$  shall be computed by dividing  $A_{\text{ave},j}$  by the volume of the test phantom (22,000 mL).

A circular region of interest centered on the transverse field of view (*not* centered on the line source) and 180 mm in diameter shall be drawn in the reconstructed image for each slice  $i$ . The number of true counts  $C_{ROI,i,j}$  for each slice  $i$  and acquisition  $j$  shall be measured. Calculate the true rates  $R_{ROI,i,j}$ :

$$R_{ROI,i,j} = \frac{C_{ROI,i,j}}{T_{acq,j}}.$$

For each slice  $i$ , calculate a fit true counting rate  $R_{Fit,i,j}$  by weighted-least-square fitting over all acquisitions at activity concentrations less than or equal to the peak NECR rate, using the following equation:

$$R_{Fit,i,j} = \frac{A_{ave,j}}{J} \sum_{k=1}^J \frac{R_{ROI,i,k}}{A_{ave,k}}.$$

where  $J$  is the total number of acquisitions with activity at or below peak NECR, and the sum is computed over each acquisition.

For each acquisition  $j$ , the relative count rate error  $\Delta r_{i,j}$  in percentage units shall be calculated by the following equation:

$$\Delta r_{i,j} = 100 \left( \frac{R_{ROI,i,j}}{R_{Fit,i,j}} - 1 \right).$$

## 6.5 Report

Report the reconstruction algorithms, methods for random and deadtime corrections, and reconstruction parameters, such as matrix dimension and image pixel size.

For each slice, tabulate the values of  $\Delta r_{i,j}$  and  $a_{eff,j}$ . Plot a graph of the highest and lowest values among the slices of  $\Delta r_{i,j}$  versus  $a_{eff,j}$ , choosing linear graphical axes. The data points may be joined to form a true continuous curve. Report the number of axial end slices skipped in the analysis, if any.

Report the maximum value of the bias  $|\Delta r_{i,j}|$  at activity values at or below  $a_{NEC,peak}$  as determined in Section 4.5.2.

## Section 7

### Image Quality, Accuracy of Corrections

#### 7.1 General

Because of the complex interplay of different aspects of system performance, it is desirable to be able to compare the image quality of different imaging systems for a standardized imaging situation that simulates a clinical imaging condition. Due to variations in the uptake of radiopharmaceuticals and inpatient sizes and shapes, it is difficult to simulate clinical imaging conditions using a phantom. For these reasons, the results of a single phantom study can only give indications of image quality for that particular imaging situation.

#### 7.2 Purpose

The purpose of this measurement is to produce images simulating those obtained in a total body imaging study with hot lesions. Spheres of different diameters are imaged in a simulated body phantom with non-uniform attenuation; activity is also present outside the scanner. Image contrast and background variability ratios for hot spheres are used as measures of image quality. In addition, the accuracy of the corrections is determined from the uniform background, and cold lung insert regions.

#### 7.3 Method

##### 7.3.1 Symbols

**Contrast ( $Q_{xxx}$ )** – the contrast of a sphere in a warm background:

- a.  $Q_H$  – hot sphere contrast

**Background variability ( $N_{xxx}$ )** – used as part of the image quality measurement:

- a.  $N_j$  – coefficient of variation for all ROIs of size  $j$  in the image volume

**Relative count error ( $\Delta C$ )** – the ratio of the measured, averaged counts in a cold lung region relative to the mean counts in the warm background and expressed as a percentage:

- a.  $\Delta C_{lung}$  – relative error in lung insert

**Standard deviation ( $SD_{xxx}$ )** – used as part of the background variability measurement:

- a.  $SD_j$  – standard deviation for all ROIs of size  $j$  in the image volume

##### 7.3.2 Radionuclide

The radionuclide for this measurement shall be  $^{18}\text{F}$ . The concentration of the background activity in the phantom shall be 5.3 kBq/mL (0.14  $\mu\text{Ci}/\text{mL}$ )  $\pm 5\%$  as calibrated at the start of imaging. This activity concentration corresponds to 370 MBq (10 mCi) per 70,000 mL, a typical injected dose for total body studies. If the manufacturer suggests a lower injected activity for total body imaging, a corresponding lower background activity concentration may be used for this study. The background activity concentration used and the manufacturer's recommended injected dose for total body imaging shall be reported. All spheres shall be filled with a concentration of four times that of the background (i.e., 4:1). The line source of the test phantom shall be filled with 116 MBq (3.08 mCi) of  $^{18}\text{F}$  to yield an effective activity "concentration" equal to the background activity concentration; if a lower background activity is used in the phantom, then a corresponding lower activity shall be used in the line source.

### 7.3.3 Source Distribution

The imaging phantom consists of four parts:

- a. a body phantom of at least 180 mm interior length, with a cross-section as shown in Figure 7-1;
- b. six fillable spheres with internal diameters of 10, 13, 17, 22, 28, and 37 mm with a wall thickness of less than or equal to 1 mm (see Figure 7-2);
- c. to simulate the attenuation of lung, a cylindrical insert filled with a low atomic number material with an average density of  $0.30 \pm 0.10 \text{ g/mL}$ , 50  $\pm 2$  mm in outside diameter with a wall thickness less than 4 mm, that is centered inside the body phantom and that extends through the entire axial extent of the phantom;
- d. the test phantom (line source in solid polyethylene cylinder) used for the scatter fraction, count losses and randoms measurement described in Section 4.

Parts (a), (b), and (c) are described in IEC Publication 61675-1, *Radionuclide Imaging Devices—Characteristics and Test Conditions. Part 1: Positron Emission Tomographs*, 1998.

The six spheres shall be filled with  $^{18}\text{F}$  for hot lesion imaging. The centers of the spheres shall be placed 70 mm from the body phantom endplate so that they are axially in the same transverse slice. The transverse positioning of the spheres shall be so that the centers of the spheres are positioned at a radius of 57.2 mm from the center of the phantom, as shown in Figure 7-2. The 17 mm diameter sphere shall be positioned along the horizontal axis of the phantom.

The body phantom shall be filled with the background activity concentration and placed on the imaging table. The body phantom shall be positioned axially in the scanner so that the center of the spheres is at the middle slice of the scanner and positioned transaxially so that the center of the phantom is centered in the scanner. The phantom shall be aligned so that the plane through the centers of the spheres is coplanar to the middle slice of the scanner to within 3 mm throughout the extent of the phantom. A 700  $\pm 5$  mm length of the line source of the test phantom shall be filled with  $^{18}\text{F}$  and threaded through the 6.4 mm hole in the test phantom. The test phantom shall then be placed at the head end of the body phantom and abutting the body phantom, as shown in Figure 7-3, in order to approximate the clinical situation of having activity that extends beyond the scanner.

The phantom shall be set on the patient table, and the patient table height shall be adjusted to center the lung insert in the body phantom in the transaxial field of view. If the patient table height is adjustable but cannot center the phantom, adjust the patient table height to center the phantom as closely as possible, and report the distance from the center of the phantom to isocenter. If the patient table height has no capacity for adjustment, report the distance from the center of the phantom to isocenter. Under no circumstances shall the phantom be elevated above the patient table surface to center the phantom.

### 7.3.4 Data Collection

The data acquisition time shall be determined considering the axial distance the patient table is translated between positions in a total body study (typically less than the axial field of view of the scanner) and the total axial imaging distance being simulated. The imaging time shall be set so as to simulate a total body scan, 100 cm total axial imaging distance, in 30 minutes of emission imaging, calculated as:

$$T = \frac{30 \text{ min}}{100 \text{ cm}} \times \text{axial step} ,$$

where *axial step* is the distance the patient table is moved between positions in a standard total body study

Additional measurements may be taken where the imaging time is increased to simulate a longer total imaging time or a decreased total axial imaging distance. For example, one may choose an imaging time

that corresponds to a total axial imaging distance of 50 cm in 30 minutes. The actual imaging times are to be reported as well as the total axial imaging distance being simulated. Because the scans have limited counts, it is recommended that three replicate scans be acquired in order to improve the reproducibility of the results. The durations of the second and third scans may be extended to account for the decay of the isotope.

### 7.3.5 Data Processing

All slices shall be reconstructed with all available corrections applied to the data. Images shall be reconstructed using the standard parameters (e.g., image matrix size, pixel size, slice thickness, reconstruction algorithm, filters, or other smoothing applied) for whole-body studies, as recommended by the manufacturer. These reconstruction parameters, along with reconstruction algorithm, methods for attenuation, scatter and random corrections, shall be reported. The data may be reconstructed using multiple methods (e.g., with and without the use of time-of-flight information, with and without detector resolution compensation) and the results reported for each method, provided the pertinent reconstruction parameters, as described above, are reported for each reconstruction method used.

## 7.4 Analysis

### 7.4.1 Image Quality

A transverse image centered on the hot spheres shall be used in the analysis. The same slice shall be used for all spheres. Regions of interest (ROIs) shall be drawn on each hot sphere. A circular ROI shall be used with a diameter equal to the inner diameter of the sphere being measured. The ROI analysis tool should take into account partial pixels and also permit movement of the ROI in increments of 1 mm or smaller.

ROIs of the same sizes as the ROIs drawn on the hot spheres shall be drawn in the background of the phantom on the slice centered on the spheres. Twelve 37 mm diameter ROIs shall be drawn throughout the background at a distance of 15 mm from the edge of the phantom but no closer than 15 mm to any sphere (an example of ROI placement is shown in Figure 7-4). ROIs of the smaller sizes (10, 13, 17, 22, and 28 mm) shall be drawn concentric to the 37 mm background ROIs. The ROIs shall also be drawn on the slices as close as possible to +2 cm, +1 cm, -1 cm and -2 cm on either side of the central slice. A total of 60 background ROIs of each size, 12 ROIs on each of five slices, shall thus be drawn. The locations of all ROIs shall be fixed between successive measurements (i.e., replicate scans). The average counts in each background ROI shall be recorded.

The percent contrast  $Q_{H,j}$  for each hot sphere  $j$  is calculated by:

$$Q_{H,j} = \frac{\left( \frac{C_{H,j}}{C_{B,j}} \right) - 1}{\left( \frac{a_H}{a_B} \right) - 1} \times 100\%,$$

where:

- a. is the average counts in the ROI for sphere  $j$ ;
- b.  $C_{B,j}$  is the average of the background ROI counts for sphere  $j$ ;
- c.  $a_H$  is the activity concentration in the hot spheres;
- d.  $a_B$  is the activity concentration in the background.

The percent background variability  $N_j$  for each sphere  $j$  is calculated as:

$$N_j = \frac{SD_j}{C_{B,j}} \times 100\%$$

where  $SD_j$  is the standard deviation of the background ROI counts for sphere  $j$ , calculated as:

$$SD_j = \sqrt{\sum_{k=1}^K (C_{B,j,k} - C_{B,j})^2 / (K - 1)},$$

where the sum is taken over the  $K=60$  background regions of interest.

#### 7.4.2 Accuracy of Corrections

A circular ROI,  $30 \pm 2$  mm in diameter, shall be centered on the lung insert. Record the average pixel value within the ROI,  $C_{lung,i}$ , for each image slice  $i$  within the lung insert region (but exclude those slices that are within 30 mm of the axial edge of the lung insert).

To measure the residual error in the corrections, the relative error  $\Delta C_{lung,i}$  in percentage units for each slice  $i$  shall be calculated as follows:

$$\Delta C_{lung,i} = \frac{C_{lung,i}}{C_{B,37\text{mm}}} \times 100\%,$$

where:

- a.  $C_{lung,i}$  is the average counts in the lung insert ROI;
- b.  $C_{B,37\text{mm}}$  is the average of the sixty 37 mm background ROIs computed in Section 7.4.1.

#### 7.5 Report

The following items are to be reported:

- a. background concentration used to fill the phantom and manufacturer's recommended injected dose for total body studies;
- b. acquisition parameters including emission imaging time, axial step size, and total axial imaging distance simulated;
- c. the method of estimating photon attenuation during the emission scan (e.g., by CT measurement, computation from the source description);
- d. the method of reconstruction, including the reconstruction filters and other smoothing, applied in both the transaxial and axial directions, and any corrections that are applied (e.g., scatter, randoms, attenuation, dead time, decay, normalization), pixel size, image matrix size, and slice thickness;
- e. the percent contrast and percent background variability for each sphere size and each concentration ratio used. If replicate scans are acquired, the average and SD of the percent contrast and percent background variability over the replicates shall be reported;
- f. the value of  $\Delta C_{lung,i}$  for each slice measured. The average of these errors shall also be reported;
- g. the transverse image through the center of all the spheres, and a coronal image through the center of the 17 mm sphere.

These items shall be specified for each set of scan conditions tested (i.e., value of  $N$  and axial scan length) and for each reconstruction method used (e.g., with and without the use of time-of-flight information, with and without detector resolution compensation).

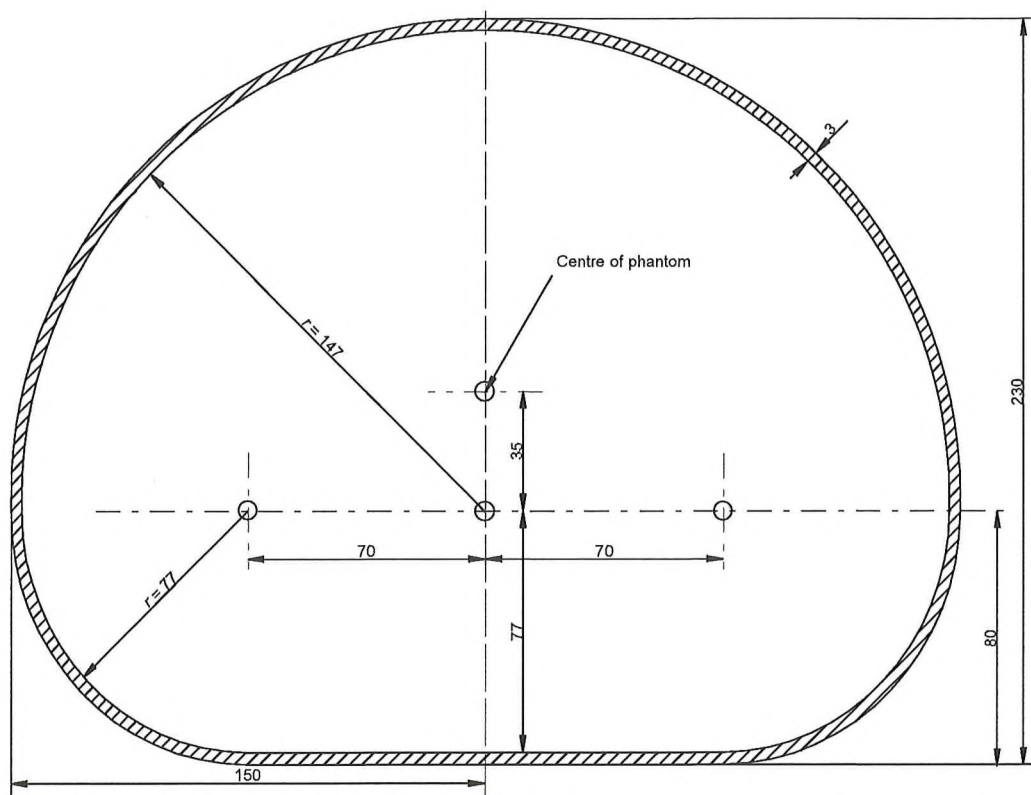


**Figure 7-1**  
**Cross-section of Body Phantom**

All dimensions are in millimeters and are given within  $\pm 1$  mm. The phantom material is polymethylmethacrylate. (From IEC Standard 61675-1; used with permission)

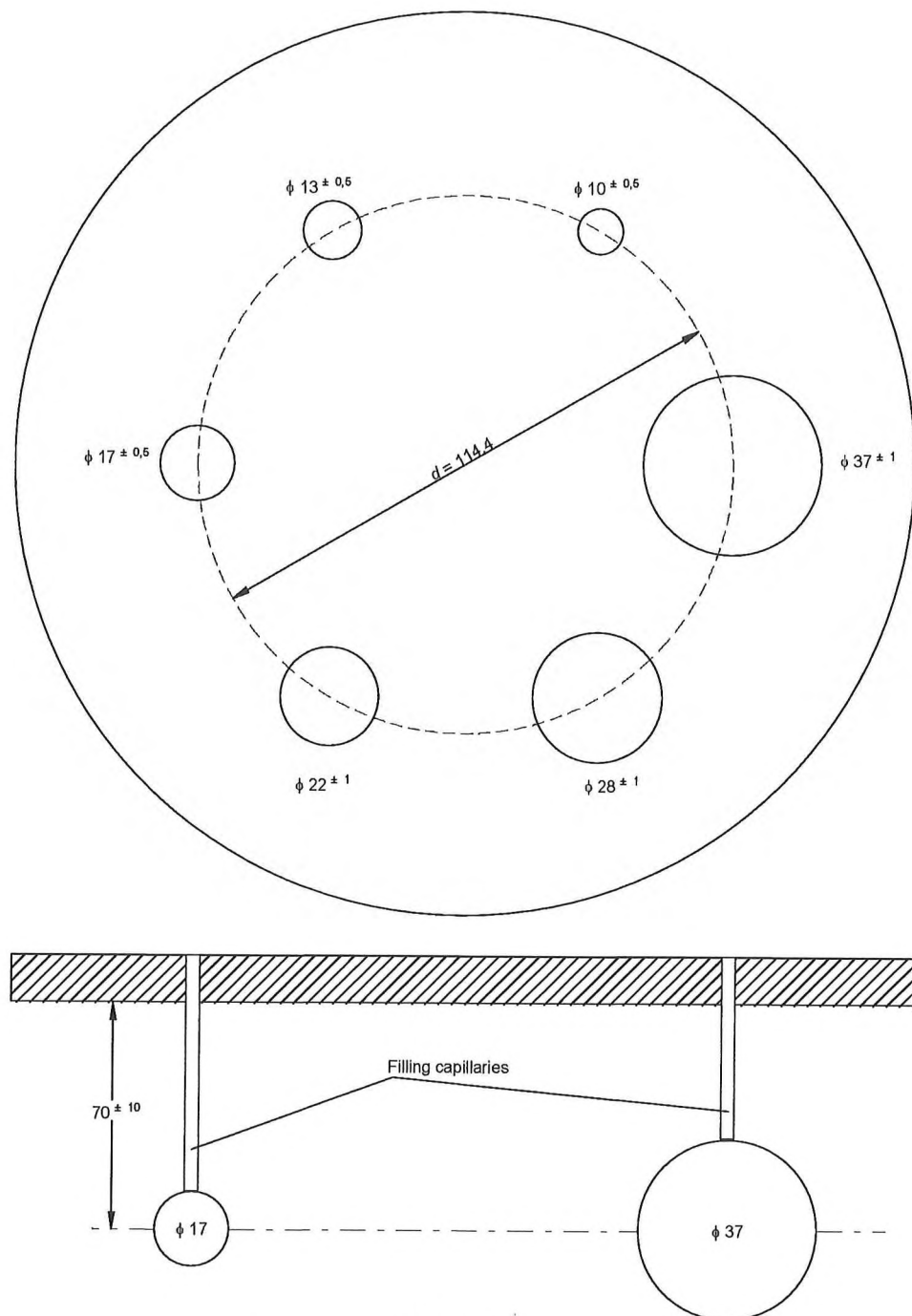


**Figure 7-2**  
**Phantom Insert with Hollow Spheres**

All diameters given are inside diameters. The wall thickness of the spheres shall be less than or equal to 1 mm. The centers of the spheres shall be  $70 \pm 10$  mm from the inside surface of the mounting plate, so they are axially all in the same transverse slice. Phantom material is polymethylmethacrylate, although the spheres may alternatively be made from glass. (From IEC Standard 61675-1; used with permission)

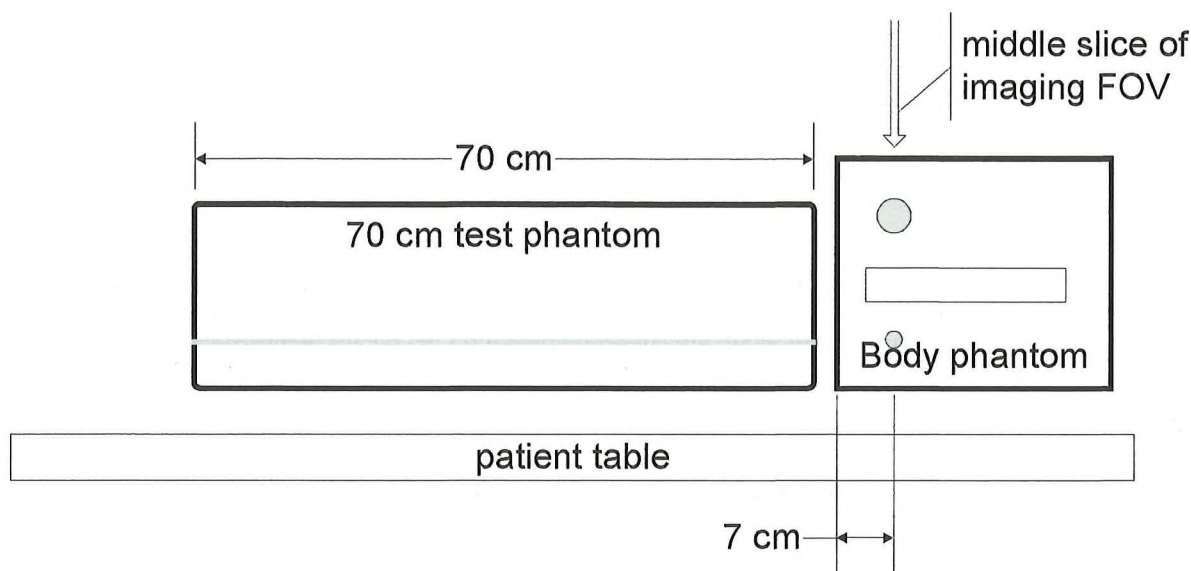


**Figure 7-3**  
**Arrangement of Radionuclide Distribution**

The test phantom shall be placed at the head end of the body phantom and abutting the body phantom in order to approximate the clinical situation of having activity that extends beyond the scanner.

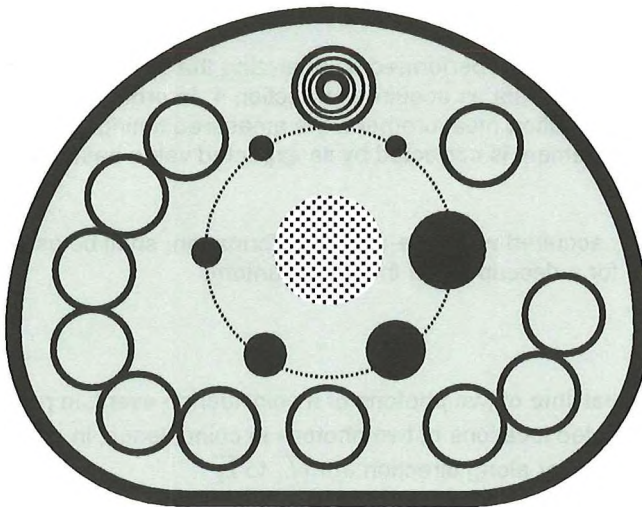


**Figure 7-4**  
**Example of Background ROI Placement for Image Quality Analysis**

Twelve 37 mm ROIs are drawn in the background region. An example of ROI placement is shown in the figure. Background ROIs for the 10, 13, 17, 22 and 28 mm features are drawn concentric to the 37 mm ROIs as indicated in the top background ROI in the figure.

## Section 8 Time-of-Flight Resolution

### 8.1 General

The time-of-flight (TOF) resolution of a system defines the uncertainty in detecting the arrival time-difference of two photons in a coincidence event. It represents the positional uncertainty of the localization of each annihilation point along the line-of-response (LOR) during reconstruction. The measurement and analysis method is based on work described in Wang G-C *et al.*, "PET Timing Performance Measurement Method Using NEMA NEC Phantom," *IEEE Transactions on Nuclear Science*, vol. 63, no. 3, 2016. pp. 1335-1342.

The measurement of TOF resolution is not applicable to any system that does not offer TOF acquisition and reconstruction modes.

### 8.2 Purpose

The purpose of this procedure is to characterize the accuracy of TOF measurement. The TOF accuracy is characterized by the full width at half-maximum amplitude (FWHM) of the detector response.

This measurement method characterizes the intrinsic time-of-flight resolution of the data produced by the scanner. It does not characterize the reconstruction process or effect of time-of-flight reconstruction on the image.

### 8.3 Method

The measurement of TOF resolution is performed by analyzing the spread of the line source in TOF dimension using the test phantom data as acquired in Section 4. In order to aggregate the data to arrive at a single, composite TOF resolution measurement, the measured timing difference for each coincidence event used in the TOF measurement is corrected by its expected value based on the measured geometry of the phantom.

The test data of Section 4.3, acquired with time-of-flight information, shall be used to measure TOF resolution. See Section 4.3 for a description of the test phantom.

#### 8.3.1 Symbols

|                        |   |
|------------------------|---|
| $t_1, t_2$             | arrival time of two photons of a coincidence event, in picoseconds  |
| $\vec{L}_1, \vec{L}_2$ | detected locations of two photons in coincidence, in millimeters  |
| $\vec{u}$              | unit vector along direction from $\vec{L}_1$ to $\vec{L}_2$   |
| $\vec{P}_1, \vec{P}_2$ | centers of the end points of the line source in image space, in millimeters                                   |
| $\vec{v}$              | unit vector along direction from $\vec{P}_1$ to $\vec{P}_2$   |
| $\vec{l}$              | point of closest approach of the LOR (as defined by $\vec{u}$ ) to the line source (as defined by $\vec{v}$ ) |
| $c$                    | speed of light (0.3 millimeters per picosecond)   |
| $t$                    | timing error accumulated in the TOF histogram $C_j(t,r)$  |
| $r$                    | distance of LOR to the line source accumulated in TOF histogram $C_j(t,r)$                                    |
| $\Delta r$             | histogram bin size in $r$ dimension   |
| $C_{L,t,j}, C_{R,t,j}$ | counts at the left and right edges, respectively, of the 40 mm wide strip at the center of $C_j(t,r)$         |

Note: that all position coordinates such as  $\vec{L}_1$  must be defined in a common coordinate system. In a hybrid imaging system ,it may be convenient to define that coordinate system in the PET detector frame of reference (i.e., not adjusting the coordinates for the alignment of the PET and anatomic imaging coordinates).

Figure 8-1 shows the geometry used in the processing and analysis of the coincidence data.

### 8.3.2 Radionuclide

The radionuclide used for this measurement shall be  $^{18}\text{F}$ . The amount of radioactivity shall be sufficient to reach the peak NECR value reported in Section 4.

### 8.3.3 Source Distribution

See subsection 4.3.3 for a description of the source distribution for this test.

### 8.3.4 Data Collection

See subsection 4.3.4 for a description of the acquisition parameters for this test.

### 8.3.5 Data Processing

For tomographs with AFOV of 65 cm or less, all data shall be considered. For tomographs with AFOV greater than 65 cm, only axial slices in the central 65 cm shall be considered. No corrections for detector sensitivity variation, detector motions such as scatter, random, deadtime or attenuation shall be applied to the measurements, except while reconstructing the images used to localize the line source in section 8.3.5.1.

#### 8.3.5.1 Identifying the Line Source Position

Figure 8-1 provides a pictorial representation of the geometry defining the calculations used in the processing and analysis of the coincidence data.

To accurately aggregate the TOF data to assess the uncertainty of its measurement, it is necessary to know the position of the line source to better accuracy than the tolerances on its location. To do this, the first frame of the dynamic sequence where the activity is below the peak NECR shall be reconstructed with all available corrections except for decay correction (allowing images reconstructed for the Count Rate Correction Accuracy test in Section 6 to be used here), and a transaxial pixel size not to exceed 2.5 mm, forming images in the PET coordinate system. The location of the line source shall be determined on all imaging planes of the scanner, except for those within 10 mm of either end of the axial field of view, by a centroid calculation. A line shall be fit to these centroid positions; the intersection of that line with the first and last axial plane of the scanner defines the points designated as  $\vec{P}_1$  and  $\vec{P}_2$ , respectively. The unit vector denoting the direction from  $\vec{P}_1$  to  $\vec{P}_2$  is defined as:

$$\vec{v} = \frac{\vec{P}_2 - \vec{P}_1}{|\vec{P}_2 - \vec{P}_1|}.$$

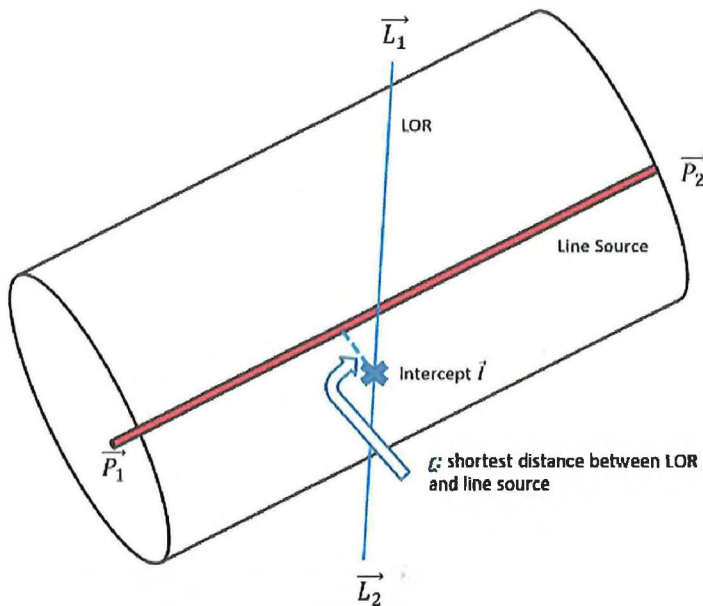


**Figure 8-1**  
**Determination of LOR Distance from Line Source**

The intercept of the LOR with the line source is defined as the point along the LOR with the shortest distance to the line source.

#### 8.4 Analysis

The following analysis is performed on each time frame of the test phantom data beginning with the last frame acquired above the peak NECR as measured in Section 4, and continuing through all frames with at least 500,000 prompt events acquired.

##### 8.4.1 2-D Histogram formation

For each coincidence event in the data set, define  $\vec{L_1}$  and  $\vec{L_2}$  (in units of millimeters) as the detected locations of the coincident photons in the PET coordinate system, as used in image reconstruction. If the LOR in the data set represents an aggregation of several different crystal pairs, then define  $\vec{L_1}$  and  $\vec{L_2}$ , as two points along the line in PET coordinates used for that LOR in image reconstruction. Then, perform the following calculations:

- compute the unit vector from  $\vec{L_1}$  to  $\vec{L_2}$ :

$$\vec{u} = \frac{\vec{L_2} - \vec{L_1}}{|\vec{L_2} - \vec{L_1}|}.$$

- compute the distance between the LOR and the line source:

$$r = (\vec{L_1} - \vec{P_1}) \cdot \frac{\vec{u} \times \vec{v}}{|\vec{u} \times \vec{v}|}.$$

If  $|r| > (20 + \Delta r)$  mm, where  $\Delta r$  is the histogram bin size along the  $r$ -dimension, this event does not contribute to the data required for the computation of timing resolution, and further processing of this event is not necessary. Note that additional margin  $\Delta r$  is to make sure that the proper interpolation can be performed at  $r = \pm 20$  mm for later random and scatter correction in Section 8.4.2.

- c. Compute the point of closest approach of the LOR to the line source:

$$\vec{I} = \vec{L}_1 + \frac{(\vec{L}_1 - \vec{P}_1) \cdot (\vec{u} - \vec{v})}{|\vec{u} \cdot \vec{v}|^2 - 1} \vec{u} .$$

- d. Compute the timing error  $t$  (in units of picoseconds) as the difference between the measured TOF data for the event and its expected TOF offset based on the point of closest approach of the line source to the LOR:

$$t = (t_1 - t_2) - \frac{|\vec{L}_1 - \vec{I}| - |\vec{L}_2 - \vec{I}|}{c} .$$

Each event is accumulated into one 2-D histogram  $C_j(t, r)$  for each acquisition  $j$ . The 2-D histograms should be centered on zero in both the  $t$  and  $r$  dimensions. The bin sizes in  $t$  and  $r$  should be less than one-quarter of the expected FWHM of the spatial and timing distributions, respectively. Since it is not required for subsequent processing, it is not necessary to retain data for which  $|r| > (20 + \Delta r)$  mm, or for which  $|t|$  is substantially greater than one-half of the expected timing FWTM.

#### 8.4.2 Scatter and Random Removal

As in Section 4.4, true events are expected to occur only in radial distance less than 20 mm from the line source, but there is a background of scattered and random coincidence events that extend beyond this 40 mm wide region. To remove scatter and randoms from the TOF offset profile, the following steps shall be performed for each timing bin  $t$  of each acquisition  $j$ :

- a. Determine the counts per pixel,  $C_{L,t,j}$  and  $C_{R,t,j}$ , at the left and right edges, respectively, of the 40 mm wide strip at the center of  $C_j(t, r)$ . If these points do not correspond to sample locations of  $C_j(t, r)$  these values are found by linear interpolation. See Figure 4-2 for a pictorial representation of this process.
- b. Form the 1D timing histogram  $C_j(t)$  by summing contributions from all radial bins in the 40 mm wide strip, corrected for the background:

$$C_j(t) = \sum_r \left\{ C_j(t, r) - \left[ \left( \frac{20 - r}{40} \right) C_{L,t,j} + \left( \frac{r + 20}{40} \right) C_{R,t,j} \right] \right\} .$$

#### 8.4.3 FWHM Analysis

For each acquisition  $j$ , the maximum value of  $C_j(t)$  shall be determined by a parabolic fit using the peak point and its two neighboring points. The FWHM shall be determined by linear interpolation between adjacent pixels at half the maximum value of the response function. This procedure is the same as is used to determine spatial resolution; Figure 3-1 is a pictorial representation of the process.

#### 8.5 Report

The following items are to be reported:

- a. TOF resolution ( $FWHM_{TOF}(j)$ ) (in units of picoseconds), plotted as a function of the average effective radioactivity concentration  $a_{ave}(j)$ , as defined in Section 1.2 where the volume  $V$  is the total volume of the cylindrical phantom (22,000 mL)
- b. TOF resolution ( $FWHM_{TOF}$ ) (in units of picoseconds) at average effective radioactivity concentration of 5.3 kBq/mL, determined by linear interpolation from the values of  $a_{ave}(j)$  immediately above and below 5.3kBq/mL.

## Section 9

### PET- CT Coregistration Accuracy

#### **9.1 General**

The alignment accuracy between PET and CT data is critical for attenuation correction as well as for localization of structures of interest. Many systems implement corrections for the mechanical offsets between the PET and CT gantries. It is important that the residual alignment error between PET and CT data is minimized, after correcting for the mechanical offsets, to ensure accurate attenuation correction and localization.

#### **9.2 Purpose**

The purpose of this measurement is to determine the coregistration error between PET and CT data. Data is acquired with PET and CT fiducial markers at 6 locations within the PET and CT field of view, with mass distributed on the patient handling system. Requirements are provided for the width of the distributions of the fiducial markers in the data. The centroids of the fiducial markers are calculated within the PET and CT data, and the coregistration error is determined by calculating the distance between the centroids.

#### **9.3 Method**

##### **9.3.1 PET-CT Fiducial Marker**

Each PET/CT fiducial marker used for this test shall meet the following requirements:

The PET portion of each fiducial marker:

- a. shall contain a PET emitting nuclide, such as  $^{18}\text{F}$  or  $^{22}\text{Na}$ , with an activity sufficiently low that at least one of the following is true:
  1. the percent dead time losses are less than five percent, or,
  2. the random coincidence rate is less than five percent of the total event rate;
- b. shall be concentric with the CT portion of the fiducial marker;
- c. shall have dimensions such that the requirements in Section 9.4.6 are met.

The CT portion of each fiducial marker:

- a. shall contain material that is greater than 500 HU (Hounsfield Units), in order for the fiducial marker container not to impact the measurement, but less than the maximum HU capable of being reproduced by the manufacturer's CT scanner in order not to saturate the CT data. This HU requirement may be achieved with CT signal-enhancing material, such as but not limited to a CT contrast solution (e.g., iopromide), or a high-density material;
- b. shall be concentric with the PET portion of the fiducial marker;
- c. shall have dimensions such that the requirements in Section 9.4.6 are met.

The fiducial markers may be generated from either separate concentric portions or from a mixture of positron emitter and CT contrast.

##### **9.3.2 Fiducial Marker and Mass Distribution**

See Figure 9-1 for a demonstration of the source and mass placement on the table.

###### **9.3.2.1 Mass on Patient Table**

Measurements shall be collected with a nominal mass of  $115\text{ kg} \pm 2.5\text{ kg}$  ( $253.5 \pm 5.5\text{ lbs.}$ ) on the patient table, distributed such that:

- a.  $50 \pm 5\%$  of the mass is evenly distributed over 65 cm, between 20 cm from the tip of the table and 85 cm from the tip of the table
- b. The remainder of the mass is evenly distributed over 65 cm, between 115 cm from the tip of the table and 180 cm from the tip of the table.

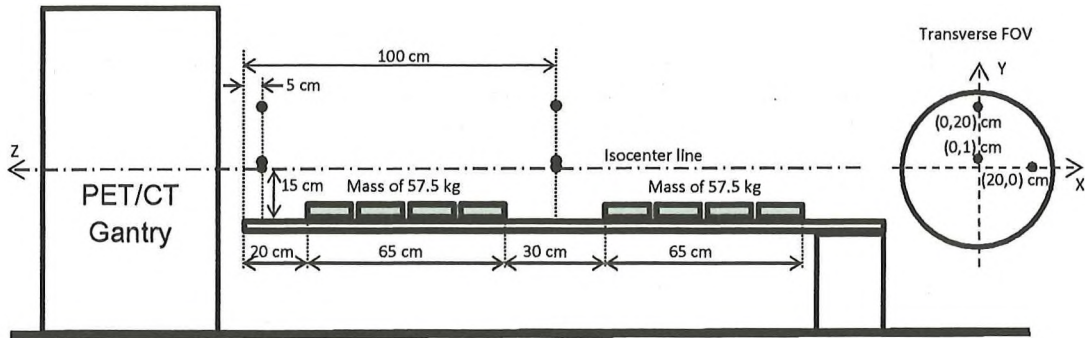


**Figure 9-1**  
**Position of Fiducial Markers and Masses on the Patient Table**

#### 9.3.2.2 Table height for All Acquisitions

For all acquisitions, the height of the patient handling system shall be fixed such that the trough of the table, at a distance  $5 \pm 2$  cm from the table tip, is located  $15 \pm 1$  cm below the center of the PET/CT transverse FOV. The system configuration (e.g., the fusion transformation between CT and PET system) shall be identical for all point source acquisitions.

#### 9.3.2.3 Location of PET/CT Fiducial Markers

The fiducial markers shall be imaged at six points, three points on each of two transaxial planes, as follows:

- a. In the transverse directions [in all cases with a positioning accuracy in the PET FOV of  $\pm 1$  cm along both X and Y, and with the coordinate system origin  $(X,Y) = (0,0)$  located at the center of the PET transverse FOV]:
  1. at a nominal location of  $(X,Y) = (0,1)$  cm (centered laterally, 1 cm offset vertically from the center of the transverse FOV),
  2. at a nominal location of  $(X,Y) = (0,20)$  cm (centered laterally, 20 cm offset vertically from the center of the transverse FOV), and
  3. at a nominal location of  $(X,Y) = (20,0)$  cm (20 cm offset horizontally from the center of the transverse FOV, centered vertically),
- b. In the axial direction [with a positioning accuracy in the PET FOV of  $\pm 1$  cm along Z, and with the coordinate system origin  $Z = 0$  located at the edge of the PET axial FOV]
  1. in the center of the PET axial FOV ( $Z = \frac{1}{2}$  PET axial FOV)
- c. At the following locations on the table:
  1.  $5 \pm 2$  cm from the tip of the patient table;
  2.  $100 \pm 2$  cm from the tip of the patient table;

#### 9.3.3 Data Collection

Data acquisition may be completed with a single fiducial marker per acquisition (six acquisitions in all) or using multiple fiducial markers per acquisition. Finer sample size may be selected than what is typically used in clinical studies in order for the fiducial marker(s) to cover several voxels/planes.

At least five hundred thousand counts per fiducial marker shall be acquired for each PET acquisition.

Additional results obtained with protocols involving table movement during acquisition may be reported, provided that the alternate methods and their parameters are described in sufficient detail to reproduce the study results.

#### 9.3.4 Data Processing

All slices shall be reconstructed using the standard reconstruction algorithm for clinical total body studies, as recommended by the manufacturer, with the following exceptions:

- a. with no attenuation correction for PET images (i.e., only non-attenuation corrected PET images shall be used for data analysis),
- b. without smoothing or apodization for PET images;
- c. with an image matrix size such that the requirements in Section 9.4.6 are met.

### 9.4 Analysis

#### 9.4.1 PET and CT Image Fusion

In order for the PET and CT data to be fused, the following must hold:

- a. The coordinate transform between the PET and CT data shall be the transform used for routine whole-body studies as produced by the standard system calibration.
- b. The PET and CT data shall be positioned in a common real-world coordinate system (in units of length).
- c. This coordinate system shall be fully specified by parameters provided in image associated standard DICOM fields, such as but not limited to:
  - (0020,0032) ImagePosition (Patient),
  - (0020,0037) ImageOrientation (Patient),
  - (0028,0030) PixelSpacing, and
  - (0018,0050) SliceThickness.
- d. The coordinate system shall not be adjusted, on an image-specific basis, based on image or external landmarks.

#### 9.4.2 Processing of Data

Processed CT data:

- a. A value of 1000 HU shall be added to the CT voxel values  $V_{CT}$  in order to represent the CT distribution without substantially negative voxel values. (i.e.,  $V'_{CT} = V_{CT} + 1000$ ).
- b. Only pixels with values above 0 HU ( $V'_{CT} > 1000$ ) in the processed CT data shall be used in the calculation of the CT centroid (see Figure 9-2).

Processed PET data:

- a. Only pixels with values above 5% of the maximum voxel value ( $V_{PET,i} > 0.05 \max(V_{PET,i})$ ) shall be used in the calculation of the PET centroid for each fiducial marker  $i$ . Define  $V'_{PET,i}$  as the processed data with those pixels below the 5% threshold set to zero (see Figure 9-3).

#### 9.4.3 Location of Maximum Voxel Value in the PET and CT Data

For each fiducial marker location  $i$ , the following locations shall be determined relative to the common coordinate system:

|  |   |
|--|---|
| $\overrightarrow{r_{\max PET,i}} = \{x,y,z\}_{\max PET,i}$ | location of the maximum voxel value in the processed PET data |
| $V'_{\max PET,i}$  | maximum voxel value in the processed PET data                 |
| $\overrightarrow{r_{\max CT,i}} = \{x,y,z\}_{\max CT,i}$   | location of the maximum voxel value in the processed CT data  |
| $V'_{\max CT,i}$   | maximum voxel value in the processed CT data                  |

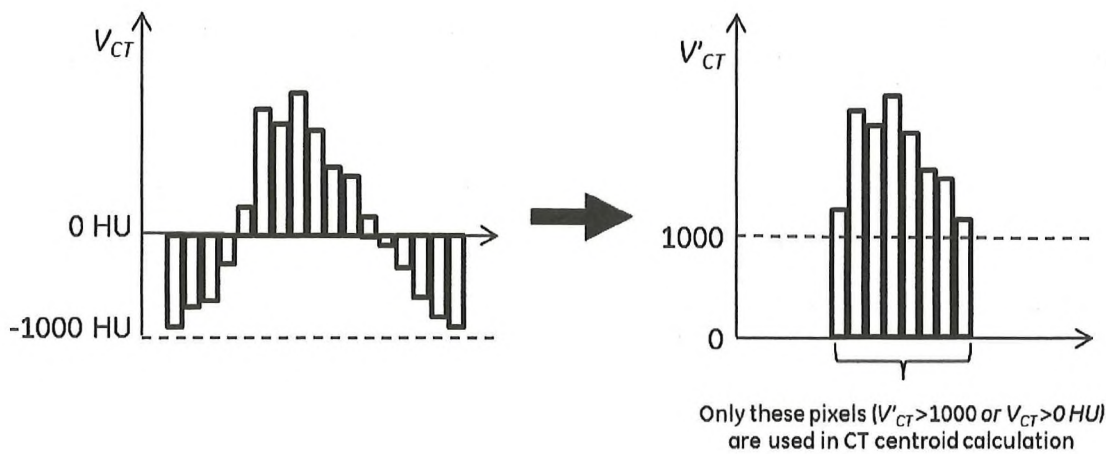


**Figure 9-2**  
Processed CT Data, Used in Centroid Calculation

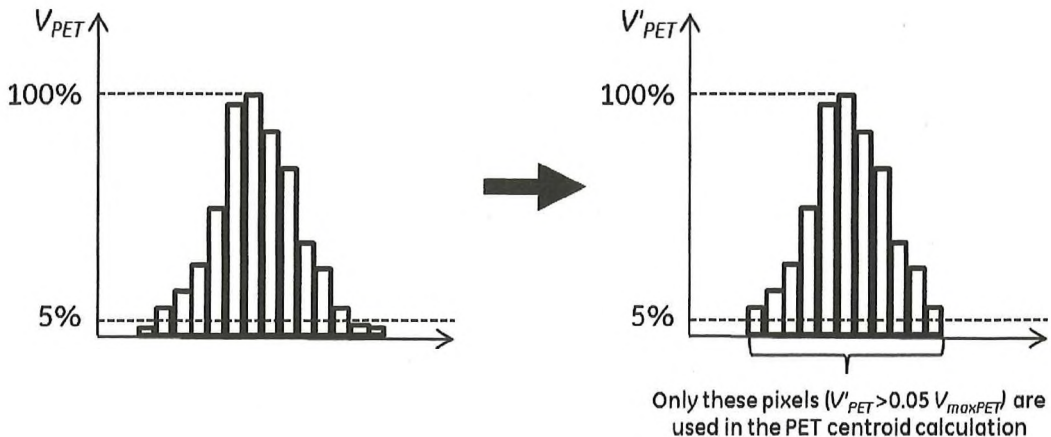


**Figure 9-3**  
Processed Pet Data, Used in Centroid Calculation

#### 9.4.4 Dimensions of the Volume Used in the Calculation of the Centroid

The purpose of this section is to determine the size of the volume of interest used to calculate the centroid.

One-dimensional response functions along profiles through the processed PET and CT data, in three orthogonal directions, through the maximum voxel value, shall be formed.

For each fiducial marker location  $i$ , the full width at half maximum ( $FWHM$ ) along each of the three orthogonal directions  $\{x,y,z\}$  shall be determined by the distance between the leftmost point above 50% of the processed maximum voxel value and the rightmost point above 50% of the processed maximum voxel value (see Figure 9-4).

$$FWHM_{\{x,y,z\}i}^{PET} = (P_{leftmost,\{x,y,z\}} - P_{rightmost,\{x,y,z\}})_i^{PET}$$

$$FWHM_{\{x,y,z\}i}^{CT} = (P_{leftmost,\{x,y,z\}} - P_{rightmost,\{x,y,z\}})_i^{CT}$$

$$FWHM_{max} = \max_{\substack{i=1,\dots,6 \\ d=\{x,y,z\}}} \{FWHM_{di}^{PET}, FWHM_{di}^{CT}\}$$

For each fiducial marker location  $i$  the volume of interest VOI shall be a cube of width equal to eight times  $FWHM_{max}$

$$VOI_{width} = 8 \cdot FWHM_{max}$$

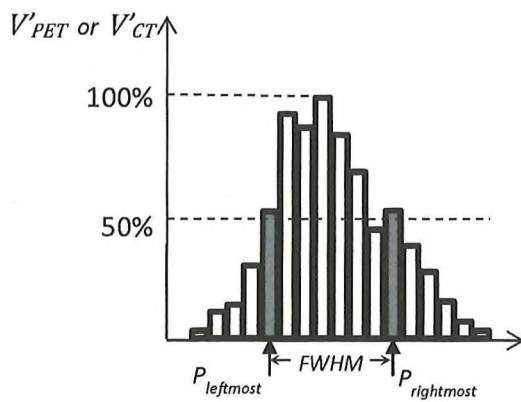


**Figure 9-4**  
**Calculation of FWHM for VOI Size Determination**

#### 9.4.5 PET and CT Centroids

For each fiducial marker location  $i$ , the volume of interest (VOI), identified in Section 9.4.4, shall be centered on  $\overrightarrow{r_{max PET,i}}$  and  $\overrightarrow{r_{max CT,i}}$ . The centroid of the fiducial marker distribution in the CT and PET data  $\overrightarrow{r_{cent CT,i}} = [x \ y \ z]_{cent CT,i}$  and  $\overrightarrow{r_{cent PET,i}} = [x \ y \ z]_{cent PET,i}$ , shall be determined as an intensity weighted sum of the voxel value  $V'_{PET,i}$  and  $V'_{CT,i}$  and their locations  $[x \ y \ z]_{PET}$  and  $[x \ y \ z]_{CT}$  within  $VOI_{width}$ .

$$[x \ y \ z]_{cent CT,i} = \frac{\sum ([x \ y \ z]_{CT,i} \cdot V'_{CT,i})}{\sum (V'_{CT,i})}$$

$$[x \ y \ z]_{cent PET,i} = \frac{\sum ([x \ y \ z]_{PET,i} \cdot V'_{PET,i})}{\sum (V'_{PET,i})},$$

where the sums in the CT calculation are performed over those voxels where  $V'_{CT,i} > 1000$ , and the sums in the PET calculation are performed over those voxels where  $V'_{PET,i} > 0.05 \max(V'_{PET,i})$  (see Figures 9-2 and 9-3).

#### 9.4.6 Verification of Fiducial Marker Dimension and Pixel Size

The purpose of this section is to verify that the fiducial marker dimensions and reconstruction pixel size are adequate to determine an accurate centroid. If the requirements below are not met, the fiducial

marker dimensions shall be increased and/or the reconstruction matrix size shall be increased (or the reconstructed pixel size decreased) until the requirements below are met.

For each fiducial marker  $i$ , one-dimensional response functions along profiles through the processed PET and CT data, in three orthogonal directions, through the voxel containing the centroid in each dimension, shall be formed, over the extent of the dimension of  $VOI_{width}$  used to calculate the centroid.

For each profile through the voxel containing the centroid in the processed PET and CT data, the maximum voxel value shall be determined:

- $\{MAX_x, MAX_y, MAX_z\}_{PET i}$  maximum voxel values along the x, the y and the z profiles in the processed PET data
- $\{MAX_x, MAX_y, MAX_z\}_{CT i}$  maximum voxel values along the x, the y and the z profiles in the processed CT data

Each ratio  $\overrightarrow{R_{CT i}} = \{R_x, R_y, R_z\}_{CT i}$  and  $\overrightarrow{R_{PET i}} = \{R_x, R_y, R_z\}_{PET i}$  of the maximum voxel value along each profile to the total number of counts along the profile, through the voxel containing the centroid over a length equal to the dimensions of the volume of interest used to determine the centroid, shall be calculated for all orthogonal directions in the processed PET and CT data. This ratio is used to verify that the fiducial marker dimensions and reconstruction pixel size are adequate to determine an accurate centroid.

$$\overrightarrow{R_{CT i}} = \left[ \frac{MAX_x_{CT i}}{\sum_x V'_{CT i}(x, y_{cent i}, z_{cent i})} \quad \frac{MAX_y_{CT i}}{\sum_y V'_{CT i}(x_{cent i}, y, z_{cent i})} \quad \frac{MAX_z_{CT i}}{\sum_z V'_{CT i}(x_{cent i}, y_{cent i}, z)} \right]$$

$$\overrightarrow{R_{PET i}} = \left[ \frac{MAX_x_{PET i}}{\sum_x V'_{PET i}(x, y_{cent i}, z_{cent i})} \quad \frac{MAX_y_{PET i}}{\sum_y V'_{PET i}(x_{cent i}, y, z_{cent i})} \quad \frac{MAX_z_{PET i}}{\sum_z V'_{PET i}(x_{cent i}, y_{cent i}, z)} \right]$$

where the sums in the equations above are over the voxels in the VOI cube for each fiducial marker  $i$ .

The maximum ratios  $R_{max CT}$  and  $R_{max PET}$  are equal to the maximum value of each ratio over each of the three dimensions {x,y,z} and each of the six fiducial marker locations:

$$R_{max CT} = \max_{\substack{i=1,\dots,6 \\ d=\{x,y,z\}}} R_{dCT i}$$

$$R_{max PET} = \max_{\substack{i=1,\dots,6 \\ d=\{x,y,z\}}} R_{dPET i}$$

The ratios  $R_{max CT}$  and  $R_{max PET}$  shall be less than or equal to 0.3 (in order for the fiducial marker to cover several pixels along each direction). If  $R_{max CT}$  or  $R_{max PET}$  are greater than 0.3, the fiducial marker dimensions and reconstruction pixel size are not adequate to determine an accurate centroid. If this is the case, the fiducial marker dimensions and/or reconstruction matrix dimensions shall be increased (or pixel size decreased) until  $R_{max CT}$  and  $R_{max PET}$  are less than or equal to 0.3.

#### 9.4.7 Coregistration Error

The coregistration error shall be calculated for each of the six fiducial marker locations  $i$ :

$$CE_i = \sqrt{(x_{cent PET i} - x_{cent CT i})^2 + (y_{cent PET i} - y_{cent CT i})^2 + (z_{cent PET i} - z_{cent CT i})^2}$$

## 9.5 Report

Report the maximum coregistration error, among the six coregistration errors.

$$MaxCE = \max(\{CE_i, i=1,\dots,6\})$$

Report the table height during data acquisition.

Confirm that the patient handling system is fixed for all acquisitions, and such that the trough of the table, at a distance  $5 \pm 2$  cm from the table tip, is positioned  $15 \pm 1$  cm below the center of the transverse FOV.

Report the maximum ratios  $R_{max\ CT}$  and  $R_{max\ PET}$ , and confirm that  $R_{max\ CT}$  and  $R_{max\ PET}$  are both less than or equal to 0.3.

§

)

)

)

**Need more?**

To obtain previous editions or additional copies of this document, please visit [www.techstreet.com/nema](http://www.techstreet.com/nema) or email [techstreet.service@clarivate.com](mailto:techstreet.service@clarivate.com)

National Electrical Manufacturers Association  
1300 North 17th Street, Suite 900 • Rosslyn, VA 22209  
[www.NEMA.org](http://www.NEMA.org)

